Clinical Utility of Novel Thrombogenicity Examination Using Whole Blood: Total Thrombus-formation Analysis System (T-TAS) in Dogs

(犬における全血での新規血栓形成能評価装置の臨床利用：全血血栓形成分析システム(T-TAS)の検討)

The United Graduate School of Veterinary Science

YAMAGUCHI UNIVERSITY

Tomoko Iwanaga

September 2021

Clinical Utility of Novel Thrombogenicity Examination Using Whole Blood: Total Thrombus-formation Analysis System (T-TAS) in Dogs

Academic Dissertation

Submitted to

The United Graduate School of Veterinary Science

Yamaguchi University, Japan

By

Tomoko Iwanaga

Department of Veterinary Medicine

Joint Faculty of Veterinary medicine

Kagoshima University, Japan

In partial fulfillment of requirements of the degree of

Doctor of Philosophy

In

Veterinary Medicine

September 2021

Major Supervisor

Professor Dr. Naoki Miura

Department of Veterinary Medicine

Joint Faculty of Veterinary medicine

Kagoshima University, Japan

Co-Supervisors

Professor Dr. Yasuyuki Endo

Department of Veterinary Medicine

Joint Faculty of Veterinary medicine

Kagoshima University

Professor Dr. Mitsuya Shiraishi

Department of Veterinary Medicine

Joint Faculty of Veterinary medicine

Kagoshima University

Associate Professor Dr. Masashi Takahashi

Department of Veterinary Medicine

Joint Faculty of Veterinary medicine

Kagoshima University

Associate Professor Dr. Kenji Baba

Department of Veterinary Medicine

Joint Faculty of Veterinary medicine

Yamaguchi University

Table of content

Chapter 2; Evaluation of antiplatelet and anticoagulant drugs with the Total Thrombus-formation Analysis System in healthy control dogs in vivo and in vitro

Chapter 3; Assess canine hemostasis with the Total Thrombus-formation Analysis System

Abstract

Blood coagulation tests cannot reflect in vivo coagulation status in one system, including platelet function, fibrin clot formation, and whole blood flow. Thus, the development for a new technique that can evaluate the blood coagulation more similar to in vivo situation is emerging in the clinical situation. Total Thrombus-formation Analysis System (T-TAS) can evaluate blood coagulation ability more resemble *in vivo* situation because the principle of T-TAS reflects on Virchow's triad. In my thesis, I evaluated the potential of the T-TAS in veterinary medicine.

In Chapter 1, I investigated the utility of the newly developed diagnostic instrument, T-TAS, for clinically healthy dogs. The T-TAS, which is a microfluidic assay that simulates conditions in vivo, measures whole blood flow at defined shear rates under conditions designed to assess platelet function (PL-chip) or coagulation and fibrin clot formation (AR-chip). The T-TAS records occlusion start time (OST), occlusion time (OT), and area under the curve (AUC). The CV of the AUC of both chips was good (CVs of 6.45% [PL] and 1.57% [AR]). The T-TAS can adapt to the evaluation of canine blood coagulation as similar to human medicine.

In Chapter 2, I evaluated the effect of antiplatelet and anticoagulant drugs in dogs by using the T-TAS. In human medicine, The T-TAS has assessed the effect of antiplatelet and anticoagulant drugs yet. I also investigated the effect of an

anticoagulation drugs; in vivo of acetylsalicylic acid and in vitro of low-molecular-weight heparin. I compared pre-and post-dose parameter values by 2-tailed paired *t*-tests using an alpha of 0.05. The inhibition of platelet function by acetylsalicylic acid was evident in the right-shift in the PL test pressure curve. The right-shift in the AR test pressure curves showed that the administration of low-molecular-weight heparin inhibited both platelets and the coagulation cascade. The T-TAS may be useful in the evaluation of canine blood coagulation and can assess the effect of these drugs in dogs.

In Chapter 3, I finally assessed canine hemostasis patients with the T-TAS. Hemorrhagic diseases are common in dogs. Current coagulation assays do not represent all aspects of in vivo hemostasis and may not predict bleeding risk. I evaluated the T-TAS in dogs with hereditary bleeding disorders and with acquired hemorrhagic syndromes (Group 1), and healthy controls (Group 2). Hereditary defects included von Willebrand disease (n=4), hemophilia A (n=2), and canine Scott syndrome (n=2). Acquired hemorrhagic disorders included neoplastic hemoperitoneum (n=2) and acute hemorrhagic diarrhea syndrome (n=1). I also procedure coagulation screening tests, fibrinogen analyses, D-dimer concentration, antithrombin activity, von Willebrand Factor antigen, PFA-100 closure time, and thromboelastography. Correlations between continuous variables were evaluated

by Spearman's rank. Continuous variables were compared between groups by Student's t-test or the Mann-Whitney U test. Alpha was set at 0.05. In combined analyses of all dogs, significant correlations were identified between T-TAS variables, between the PFA-CT and PL-chip parameters, and between TEG variables and AR-chip parameters. The prothrombin time correlated with the AR-chip AUC at both shear rates. In Group 1 dogs, the AR-chip AUC at low shear was significantly reduced compared with Group 2 dogs. Distinct patterns of aberrant thrombus formation were seen in video images recorded from dogs with von Willebrand disease and hemophilia A. The T-TAS AR-chip analysis distinguished dogs with bleeding risk compared to healthy controls. Initial evaluations of the T-TAS suggest it may aid characterization of hemostasis in patients at-risk of bleeding and assist with delineating bleeding phenotypes.

In conclusion, the T-TAS can evaluate blood coagulation in dogs, the T-TAS may be added to existing blood coagulation tests to be able to know more detail of blood coagulation status from now on.

General Introduction

The blood coagulation is a critical system for life saving hemostasis to preventing the bleeding, in terms of blood loss. In other side, if excessive accelerating coagulation occur, extra thrombi formed in small blood vessels. Such extra thrombus formation also leads the life threshing problems results in multiple organs failure. Therefore, the blood coagulation system consists in a fine balance when the bleeding is happened. The actual fine regulation in the blood coagulation system is a complicated process.

In 1960s, the model of coagulation cascade proposed by MacFarlane et al [1]. In case of the model of coagulation cascade, sequential enzyme activities happen and gradually accelerate the reaction, following the great magnification to make effective thrombus (Figure 0a). There are 3 pathways, intrinsic, extrinsic, and common pathway. The intrinsic pathway is started by Factor Ⅻ (FⅫ), the extrinsic is started by Tissue Factor (TF) and Factor Ⅶ (FⅦ), and the intrinsic and the extrinsic pathways coalesce into common pathway which ultimately produce a fibrin clot. Based on this model, two major clinical tests are developed and widely used in the clinical laboratory. The intrinsic pathway indicates the activated partial thromboplastin time (aPTT), the extrinsic pathway indicates the

prothrombin time (PT), and the common pathway is reflected by aPTT, PT and fibrin test.

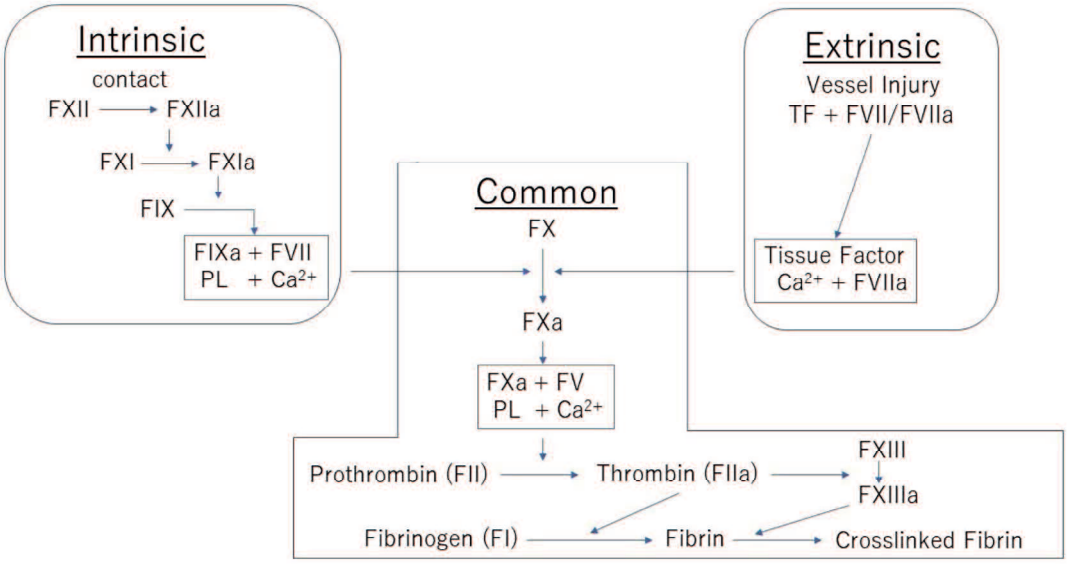

Figure 0a:

The cascade model of coagulation. The intrinsic pathway is started by Factor Ⅻ (FⅫ), the extrinsic is started by Tissue Factor (TF) and Factor Ⅶ (FⅦ), and the intrinsic and the extrinsic pathways coalesce into common pathway which ultimately produce a fibrin clot. Redesign from reference 26

The model of coagulation cascade, however, consists only in vitro, and it does not reflect in vivo. Although the intrinsic pathway and the extrinsic pathway act separately in the cascade model, this concept is conflicting because both pathways interact in the nature (in the blood vascular). For example, in case of hemophilia A and B, hemostasis occurs in patients in spite that the extrinsic pathway is normal. Moreover, this model does not include the function of platelets. Therefore,

I know that this model is not able to explain well about the coagulation reaction in vivo. Recently, the cell-based coagulation model is suggested because hemostasis in vivo occurs through assembly of coagulation factor complexes on the surfaces of activated platelets and tissue factor-bearing cells (Figure0b)[1-4] .

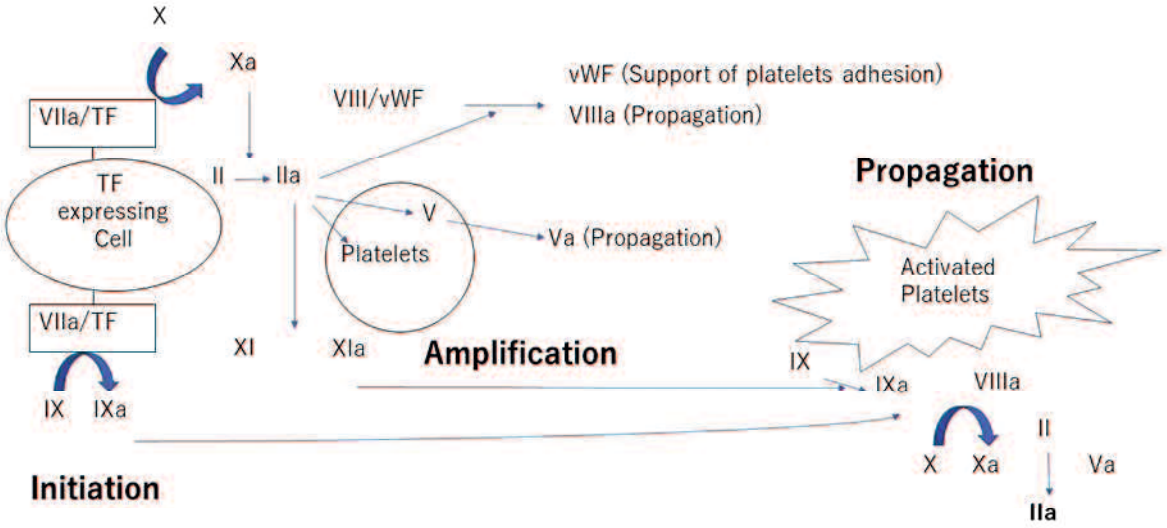

Fig 0b:
The cell-based model of coagulation. The three phases of coagulation occur on different cell surfaces: Initiation on the tissue factor-bearing cell; Amplification on the platelet as it becomes activated; and Propagation on the activated platelet surface. Redesign reference 2

Consider the coagulation reaction both cascade model and cell-based model, blood coagulation is complicated reaction. In true nature, there are many factors which include coagulation factor, anticoagulation factor, cell membrane, platelets, and even more known or unknown factors. Thus, hemostasis classification into 3

phases, primary hemostasis, secondary hemostasis, and fibrinolysis. The primary hemostasis reflects the function of platelets including von Willebrand factor (VWF). The secondary hemostasis indicates sequential reactions represented in the coagulation cascade. Fibrinolysis indicates an activity of mainly plasma anticoagulant proteins, which are critical negative regulators of coagulation. Clinically, there are many hemostasis tests which are based on these clinical hemostasis classification, primary hemostasis, secondary hemostasis, and fibrinolysis. Most of these clinically hemostasis tests examine only the coagulable factor. However, the blood coagulation is affected by blood vessels, blood flow, and coagulable state of blood cell components according to the Virchow triad. The whole blood viscoelastic tests, which include thromboelastography (TEG), thromboelastometry (ROTEM) and dynamic viscoelastic coagulometry (Sonoclot) were developed to address some of these shortcoming [5,6] and may aid in predicting bleeding risk [7]. However, these viscoelastic tests could not reflect platelet function disorders [8,9], blood flow and shear stress [10].

The Total Thrombus-formation Analysis System (T-TAS: Fujimori Kogyo Zacros, Tokyo, Japan), which is developed based on the Virchow Triad, mimics damaged blood vessels and uses microfluidic chips with collagen applied on the microducts and is performed under flow conditions using microfluids. Moreover, The T-TAS

can change shear stress to assume both artery and vein, respectively. The designed to assess platelet function or coagulation and fibrin clot formation on time [11]. Hence, the T-TAS assesses blood coagulation status under closer to in vivo conditions than other conventional coagulation tests [11-13]. The T-TAS employs 2 microfluidic chips: one is a platelet chip (PL chip), which can evaluate platelet function; the other is an atheroma chip (AR chip), which can evaluate coagulation and fibrin clot formation with platelet function. These chips permit the evaluating of the primary and secondary coagulation systems, respectively. The chips employ microduct(s) that are coated with collagen (PL chip) or collagen and thromboplastin (AR chip); the microduct(s) imitate the injured vascular wall. During the assessment, injection of whole blood into the microduct at certain shear rates (12 μL/min for PL; 10 μL/min for AR) induces the formation of a thrombus. The T-TAS measure the pressure which increase gradually reflect to thrombus form and capture the images on the microduct during thrombus formation by video recording (Fig 0c). The T-TAS enables quantitative analysis of the timing, extent and rate of thrombus formation and is equipped with a video microscope for real-time imaging and qualitative analyses [14].

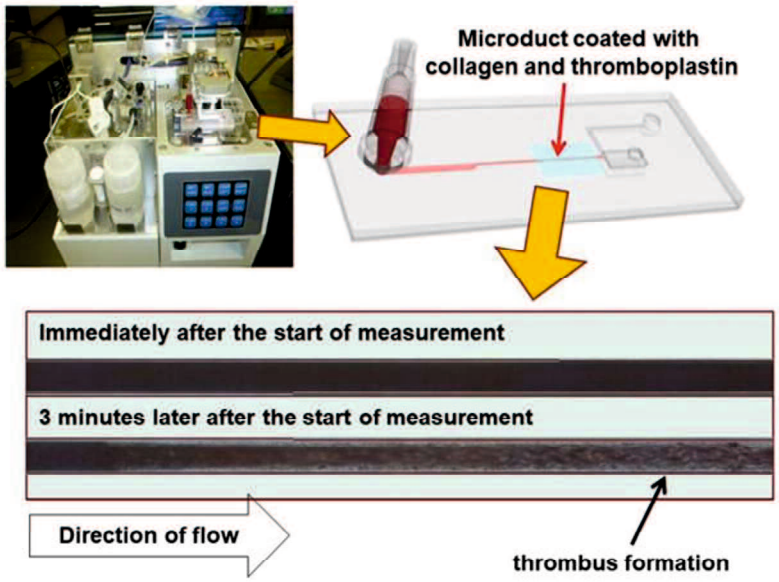

Fig 0c:

Principles of the Total Thrombus-formation Analysis System (T-TAS). **A.** Thrombus formation occurs in this microduct chamber after the injection of whole blood at certain shear rates (12 μL/min for platelet [PL]; 10 μL/min for atheroma [AR]). Microduct is coated with collagen (PL chip) or collagen and thromboplastin (AR chip).

In human medicine, the T-TAS has been used extensively to assess the effects of antithrombotic drugs [12,15], including oral direct Factor Xa inhibitors [16] and antiplatelet agents [17-19]. Studies of patients with coronary artery disease treated with various antithrombotic therapies suggest the T-TAS can predict bleeding risk [20,21]. Consistent with its ability to detect impaired thrombus formation due to antiplatelet drug therapy, the T-TAS is also sensitive to some inherited platelet function disorders. Patients with platelet storage pool disease

(characterized by a reduction in the number or content of alpha granules or dense granules) have decreased thrombus formation in the PL-chip assay, at both low and high shear[14]. In patients with von Willebrand's disease (VWD), the T-TAS appears to be sensitive to moderate to severe plasma von Willebrand factor (VWF) deficiency and the absence of large molecular weight VWF multimers [22]. Samples from patients with severe type 1 VWD, defined as VWF antigen (VWF:Ag) below 10U/dL, and those with type 2 VWD (absence of large VWF multimers), failed to occlude either AR- or PL-chips, in contrast, the occlusion times are normal in patients with milder type 1 VWD. Another study of type 1 VWD, patients with relatively prolonged occlusion time in PL-chip T10 had lower VWF levels [23]. Moreover, PL-chip T10 values correlated with bleeding scores and bleeding severity, suggesting that the T-TAS may aid prediction of bleeding risk among patients with type 1 VWD. The T-TAS can identify hemostatic abnormalities due to coagulation factor deficiencies [24] and essential thrombocythemia[25] as well.

To the best of my knowledge, no published data evaluates the utilities of the T-TAS in canine blood coagulation. In my thesis, I evaluated the utility of the T-TAS in healthy control dogs in chapter 1. Then, I investigated the potential of the T-TAS to evaluate the effect of an antiplatelet drug and an anticoagulant drug in

healthy control dogs in chapter 2. Finally, I evaluated the clinical utility of the T-TAS using canine patients with clinical bleeding disorders and investigated the potential of the T-TAS as a clinical test for canine blood coagulation.

Chapter 1

Analysis of blood clotting with the Total Thrombus-formation Analysis System in healthy control dogs

1. Abstract

The Blood coagulation is complicated and the T-TAS can evaluate blood coagulation to close in vivo because it is based on Virchow's triad. To date, coagulation tests are unable to reflect in vivo coagulation status in the same system, including platelet function, fibrin clot formation, and whole blood flow. The Total Thrombus-formation Analysis System (T-TAS), which is a microfluidic assay that simulates conditions in vivo, measures whole blood flow at defined shear rates under conditions designed to assess platelet function (PL-chip) or coagulation and fibrin clot formation (AR-chip). The T-TAS records occlusion start time (OST), occlusion time (OT), and area under the curve (AUC). I evaluated this test in healthy control dogs. The CV of the AUC of both chips was good (CVs of 6.45% [PL] and 1.57% [AR]). The T-TAS may be useful in the evaluation of canine blood coagulation.

2. Introduction

Blood coagulation is a complicated process, incorporating 3 separate systems: platelets are involved in primary hemostasis, coagulation factors are involved in secondary hemostasis, and those 2 steps are followed by fibrinolysis in tertiary hemostasis. There has been an increasing focus on blood coagulation systems in veterinary medicine[5-7,9,26,27]. Patients with hemostatic disorders (e.g., congenital bleeding diseases such as von Willebrand disease, hepatic failure, and disseminated intravascular coagulation) have a tendency to bleed. On the other hand, patients with thrombotic disorders (e.g., immune-mediated diseases, such as immune-mediated hemolytic anemia; hypoproteinemias, such as protein-losing enteritis or protein-losing nephropathy; and Cushing syndrome) exhibit excessive clot formation.

According to the Virchow triad, the stasis of blood flow, vascular wall injury, and coagulable state each influence blood coagulation. However, almost all current blood coagulation tests address only the coagulable state. For dogs, few tests can measure both primary hemostasis (based on platelets) and secondary hemostasis (based on coagulation factors)[8,26,27]. None of the existing tests assess blood flow, which is one of the most important factors in blood coagulation. Thus, the existing tests do not permit the complete evaluation of canine blood

coagulation. The Total Thrombus-formation Analysis System (T-TAS; Fujimori Kogyo Zacros, Tokyo, Japan), which is developed based on the Virchow triad, mimics damaged blood vessels and uses microfluidic chips with collagen applied on the microducts and is performed under flow conditions using microfluids. Hence, the T-TAS assesses blood coagulation status under closer to in vivo conditions than do conventional coagulation tests[11,12,28]. The use of the T-TAS has been reported in human congenital bleeding diseases (e.g., von Willebrand disease and congenital diseases that result in abnormal platelets, such as Glanzmann disease) [14,22,23,29] and in the evaluation of some antiplatelet and anticoagulant drugs[16,28,30]. The T-TAS has also been used in a canine model of atrial fibrillation[31,32].

3. Ethics statement

This study was conducted in accordance with the Ethical Code of Animal Experiment of Kagoshima University (Approval VM17021).

4. Material and Method

Animals

I collected whole blood from 7 healthy control dogs (2 Labrador Retrievers, 3 Beagles, 2 mixed breeds; 1 male, 2 castrated males, 4 spayed females; ages 1–10 y [median: 2 y, mean: 4.3 y]). The control dogs were clinically healthy and had normal complete blood counts (CBCs).

Blood sampling

The dogs were not under treatment with any drugs. All blood samples were collected from a jugular vein using a 23-ga needle and 2.5-mL syringe (Terumo, Tokyo, Japan) and were tested within 3 h.

Evaluation of thrombus formation under flow conditions (Total Thrombus-formation Analysis System; T-TAS)

The T-TAS employs 2 microfluidic chips: one is a platelet chip (PL chip), which can evaluate platelet function; the other is an atheroma chip (AR chip), which can evaluate coagulation and fibrin clot formation and is also affected by platelet function. These chips permit the testing of the primary and secondary coagulation systems, respectively. The chips employ microducts that are coated with collagen

(PL chip) or collagen and thromboplastin (AR chip); the microducts imitate the injured vascular wall. Injection of whole blood into the microduct at certain shear rates (12 μL/min for PL; 10 μL/min for AR) induces the formation of a thrombus. The T-TAS tests the pressure within the microduct during thrombus formation by video recording (Fig. 1A).

For the PL chip, I collected whole blood with hirudin (1.5% final concentration) as the anticoagulant; 350 μL of hirudin blood was loaded onto a collagen-coated PL chip at a flow rate of 12 μL/min. For the AR chip, I collected whole blood with citrate (3.13% final concentration) and danaparoid (0.5 IU/mL final concentration) as the anticoagulants. In mice and dogs, it is necessary to add danaparoid, the main component of which is heparan sulfate, which exists endogenously in the bloodstream, as an anticoagulant because citric acid alone can create a very small clot in the microducts and affect the formation of a thrombus. The citrate–danaparoid blood (480 μL) was combined with 20 μL of corn trypsin inhibitor (CaCTI), and the resulting mixture was loaded onto a collagen- and thromboplastin-coated AR chip at a flow rate of 10 μL/min. T-TAS parameters included occlusion start time (OST), occlusion time (OT), and area under the pressure curve (AUC; Fig. 1B, 1C). I defined OST as the time at which the pressure reached 10 kPa, and the OT as the time to reach 60 kPa (PL chip) or 80 kPa (AR

chip). The measurement was completed when the sample reached OT, or (in the absence of occlusion) an assay endpoint of 10 min (PL chip) or 30 min (AR chip). The AUC was calculated for the interval from the OST through the end of the assay (10 min for PL; 30 min for AR).

5. Result

In the group of 7 healthy control dogs, the means ± SDs of OST, OT, and AUC for the PL chip were 2.26 ± 0.81 min, 4.73 ± 1.21 min, and 407 ± 54, respectively; the values for the AR chip were 5.02 ± 1.83 min, 6.04 ± 2.14 min, and 1955 ± 54, respectively (Table 1a). I measured the same samples from each healthy control dog twice and calculated the CV of these parameters to confirm the differences between individuals. The CVs for the PL and AR chips were: OST, 10.9% and 10.0%; OT, 15.4% and 7.6%; and AUC, 6.4% and 1.6%, respectively (Table 1b).

6. Discussion

The blood of all dogs tested exhibited occlusion within the defined time limit (PL, 10 min; AR, 30 min), yielding precise AUCs, with relatively low variances. Notably, AUCs were relatively stable among the parameters, with CVs of AUCs of <10% for both PL and AR chips. These results suggested that the T-TAS could be used to provide measurements of canine blood coagulation, given that the AUC measures the total process of coagulation: from start of occlusion to finished occlusion in the microduct.

There are some limitations to our study. I measured baseline parameters in only 7 healthy control dogs.

7. Conclusion

I evaluated this test in healthy control dogs. I confirmed that the CV of all parameters were good. Particularly, the CV of the AUC of both chips was good (CVs of 6.45% [PL] and 1.57% [AR]). The results suggests that the T-TAS is useful for the blood coagulation examination of the dog.

8. Figures and Tables

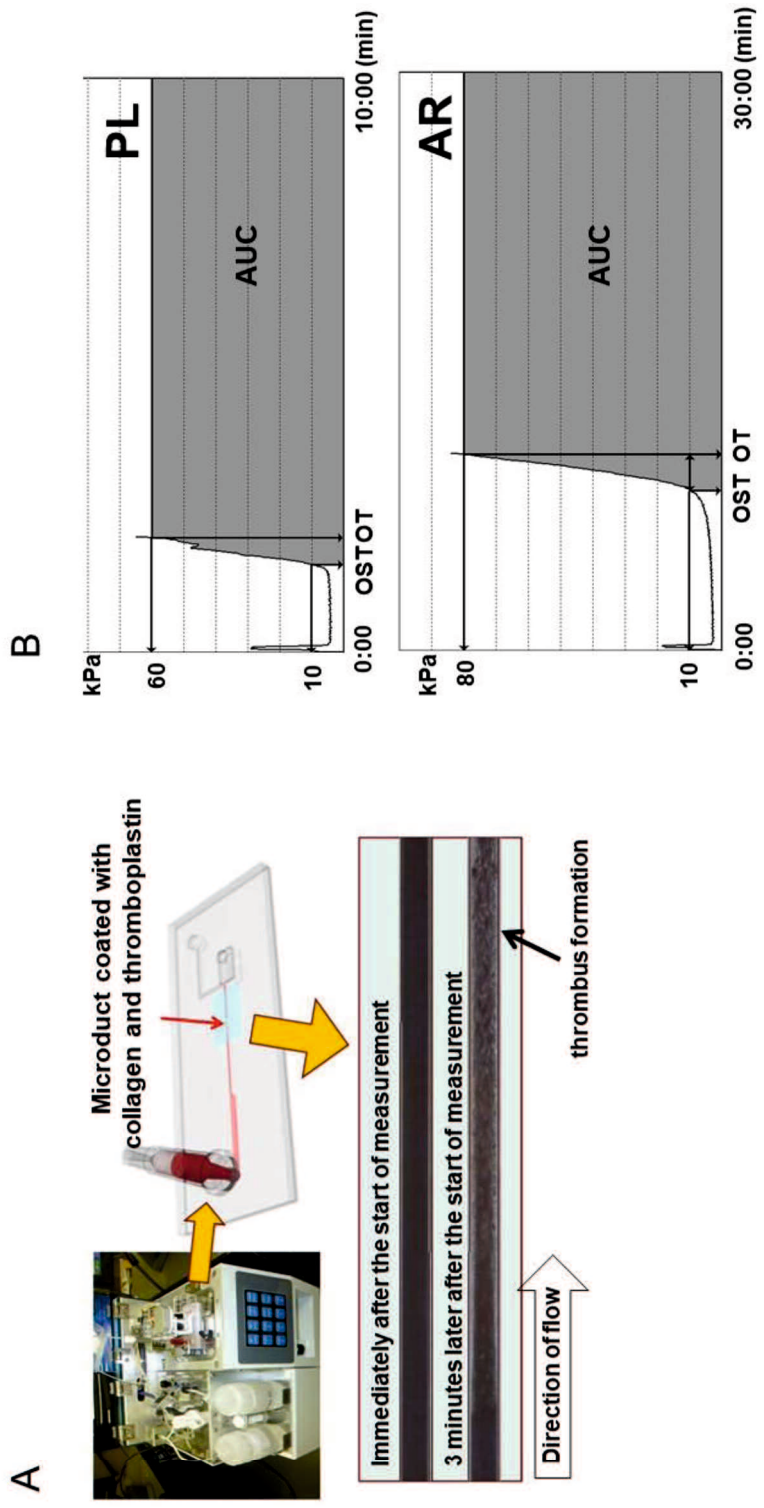

Figure 1. Principles of the Total Thrombus-formation Analysis System (T-TAS). **A.** Thrombus formation occurs in this microduct chamber after the injection of whole blood at certain shear rates (12 μL/min for platelet [PL]; 10 μL/min for atheroma [AR]). Microduct is coated with collagen (PL chip) or collagen and thromboplastin (AR chip). **B.** The T-TAS measures pressure during formation of a thrombus in the microduct and evaluates the occlusion start time (OST, i.e., the time at which pressure of 10 kPa is achieved); the occlusion time (OT; i.e., the time at which pressure of 60 kPa [PL] or 80 kPa [AR] is achieved); and the area under the pressure curve (AUC). The assay end times were 10 min (PL) or 30 min (AR).

Table 1a. The reference range of the healthy control dogs.

	OST (min)	OT (min)	AUC
PL	2.26±0.81	4.73±1.21	407±54
AR	5.02±1.83	6.04±2.14	1955±54

Table 1b. The CVs for PL and AR (%).

%	OST	OT	AUC
PL	10.9	15.4	6.4
AR	10	7.6	1.6

Chapter 2

Evaluation of antiplatelet and anticoagulant drugs with the Total Thrombus-formation Analysis System in healthy control dogs in vivo and in vitro

1. Abstract

In human medicine, the T-TAS has assessed the effect of antiplatelet and anticoagulant drugs yet. I also investigated the effect in vivo of acetylsalicylic acid (ASA), and the effect in vitro of an anticoagulation drug (dalteparin; low-molecular-weight heparin; LMWH). I compared pre- and post-dose parameter values by 2-tailed paired t-tests using an alpha of 0.05. The inhibition of platelet function by ASA was evident in the right-shift in the PL test pressure curve. The right-shift in the AR test pressure curves showed that the administration of LMWH inhibited both platelets and the coagulation cascade. The T-TAS may be useful in the evaluation of canine blood coagulation and can assess the effect of these drugs in dogs.

2. Introduction

In human medicine, the T-TAS could evaluate the effect of some drugs which are antiplatelet and anticoagulant drugs in vitro[16,18,28] and some patients who are administrated antiplatelet and anticoagulant drugs in vivo[15,30,33]. However, the T-TAS has not been used to test the ability of the analyzer to detect inhibition with in vivo or in vitro drugs in dogs. I evaluated the T-TAS assessment of clotting of blood from healthy control dogs and assessed the in vivo effect of acetylsalicylic acid (ASA), a nonsteroidal anti-inflammatory drug that inhibits platelet aggregation, and the in vitro effect of an anticoagulation drug, dalteparin sodium (low-molecular-weight heparin [LMWH]).

3. Ethics statement

This study was conducted in accordance with the Ethical Code of Animal Experiment of Kagoshima University (Approval VM17021).

4. Material and Method

I measured the effect of ASA (sulfate salt; Bufferin combination tablet A81; Eisai, Tokyo, Japan) to assess whether the PL chip could detect platelet inhibition. I administered ASA (0.5 mg/kg, q24h, PO) to 3 healthy Beagles and collected blood after 2 days of administration; the blood was assessed using both AR and PL chips.

I next measured the in vitro effect of LMWH to determine whether the AR chip could detect selective changes in secondary hemostasis (i.e., in coagulation and fibrin clot formation). I collected whole blood from 3 healthy control dogs, added dalteparin sodium (5,000 IU/5 mL; Fragmin; Pfizer Japan, Tokyo, Japan) at 2.0 IU/mL, and tested the samples on both AR and PL chips at 10 min after the addition of dalteparin.

Blood sampling

The control dogs were clinically healthy and had normal complete blood counts (CBCs). The dogs were not under treatment with any drugs. All blood samples were collected from a jugular vein using a 23-ga needle and 2.5-mL syringe (Terumo, Tokyo, Japan) and were tested within 3 hours.

Evaluation of thrombus formation under flow conditions using the T-TAS.

The T-TAS employs 2 microfluidic chips: one is a platelet chip (PL chip), which can evaluate platelet function; the other is an atheroma chip (AR chip), which can evaluate coagulation and fibrin clot formation and is also affected by platelet function. These chips permit the testing of the primary and secondary coagulation systems, respectively. The chips employ microducts that are coated with collagen (PL chip) or collagen and thromboplastin (AR chip); the microducts imitate the injured vascular wall. Injection of whole blood into the microduct at certain shear rates (12 μL/min for PL; 10 μL/min for AR) induces the formation of a thrombus. The T-TAS tests the pressure within the microduct during thrombus formation by video recording (Chapter 1, Fig. 1A).

For the PL chip, I collected whole blood with hirudin (1.5% final concentration) as the anticoagulant; 350 μL of hirudin blood was loaded onto a collagen-coated PL chip at a flow rate of 12 μL/min. For the AR chip, I collected whole blood with citrate (3.13% final concentration) and danaparoid (0.5 IU/mL final concentration) as the anticoagulants. The citrate–danaparoid blood (480 μL) was combined with 20 μL of corn trypsin inhibitor (CaCTI), and the resulting mixture was loaded onto a collagen- and thromboplastin-coated AR chip at a flow rate of 10 μL/min. T-TAS parameters included occlusion start time (OST), occlusion time (OT), and area

under the pressure curve (AUC; Chapter 1, Fig. 1B). I defined OST as the time at which the pressure reached 10 kPa, and the OT as the time to reach 60 kPa (PL chip) or 80 kPa (AR chip). The measurement was completed when the sample reached OT, or (in the absence of occlusion) an assay endpoint of 10 min (PL chip) or 30 min (AR chip). The AUC was calculated for the interval from the OST through the end of the assay (10 min for PL; 30 min for AR).

Statistical analysis

I compared pre- and post-dose parameter values by 2-tailed paired *t*-tests using an alpha of 0.05.

5. Result

Compared to control (pre-treatment) specimens, samples from animals treated with ASA exhibited right-shifts in the waveforms of PL parameters. In contrast, the waveforms of AR parameters were essentially unchanged. The right-shift of the waveform in the PL test indicates delayed occlusion as a result of suppression of platelet aggregation (Fig. 1A). I compared pre- and post-dose parameter values by 2-tailed paired *t*-tests using an alpha of 0.05. For PL parameters, pre- and post-dose values did not differ significantly for each parameter, but all alphas of PL parameters were <0.1; PL-OST ($p = 0.093$), PL-OT ($p = 0.063$), and PL-AUC ($p = 0.085$); AR-OST ($p = 0.316$), AR-OT ($p = 0.583$), and AR-AUC ($p = 0.467$; Fig. 2). These observations suggested that the T-TAS may be able to evaluate changes resulting from in vivo inhibition of platelet function alone, as expected after administration of ASA.

I next measured the in vitro effect of LMWH to determine whether the AR chip could detect selective changes in secondary hemostasis (i.e., in coagulation and fibrin clot formation). Compared to control samples, whole blood treated with dalteparin exhibited right-shifts in the waveforms of AR parameters. In contrast, the waveforms of PL parameters were essentially unchanged upon treatment. The right-shift of the waveform in the AR test indicates delayed occlusion as a result

of suppression of coagulation (Fig. 1B). I compared pre- and post-dose parameter values by 2-tailed paired *t*-tests using an alpha of 0.05. For AR parameters, there was a significant difference between pre- and post-dose values only in AR-OT (p = 0.045). But alphas of other parameters, including AR-OST (p = 0.090) and AR-AUC (p = 0.058), were <0.1. Conversely, pre- and post-dose did not differ significantly for 2 of the 3 PL parameters, yielding p = 0.157 (PL-OST) and p = 0.184 (PL-OT), although a significant difference was seen for PL-AUC (p = 0.033; Fig. 3). These observations suggested that the T-TAS may be able to evaluate changes resulting from in vitro inhibition of coagulation and fibrin clot function alone, as expected after administration of dalteparin. However, it is possible that platelets were influenced by dalteparin, given the observed significant change in PL-AUC when comparing pre- and post-administration values.

6. Discussion

In both drug effect experiments, I proposed that the T-TAS may be able to show a tendency of ASA to suppress platelet function and of LMWH to suppress coagulation and fibrin clot formation. However, I found no significant differences in our in vivo ASA study. This unexpected result may be due to the variability in the data after ASA administration, and the type II error because of the small sample size in our assay. Regarding our LMWH test, although the PL-OT and PL-OST did not differ significantly pre- and post-LMWH addition, PL-AUC was significantly altered. PL-OST is dependent on the onset of platelet thrombus formation; PL-AUC may reflect the overall stability of the platelet thrombus, which may be affected by the fibrin clot[13]. Therefore, I speculated that a LMWH affected PL-AUC only. Our results indicated that the T-TAS may be of use in evaluating the effects of antiplatelet and anticoagulant drugs in dog blood, as has been shown with human blood[15,16,18,28,30,33].

There are some limitations to our study. The effects of anticoagulation drugs in only 3 dogs. I could not exclude type II error in our assay; increased sample size is needed in future studies. Additionally, the evaluation of a LMWH was performed only in vitro.

7. Conclusion

The inhibition of platelet function by ASA was evident in the right-shift in the PL test pressure curve. The right-shift in the AR test pressure curves showed that the administration of LMWH inhibited both platelets and the coagulation cascade. The T-TAS may be useful in the evaluation of canine blood coagulation, and the T-TAS may assess of effect of antiplatelet and anticoagulant drugs.

8. Figures

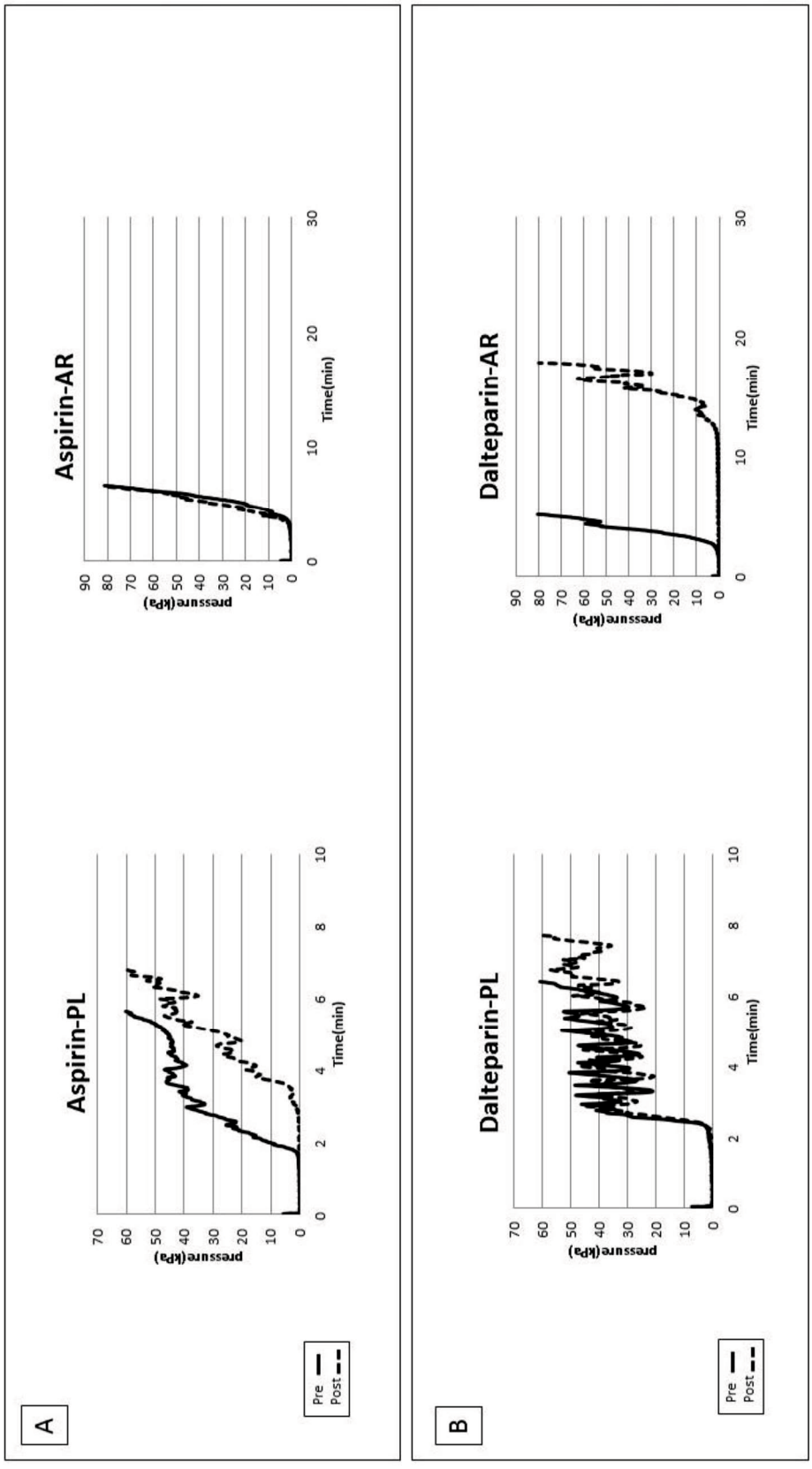
A
Aspirin-AR
Aspirin-PL
Pre
Post
pressure(kPa)
Time(min)
B
Dalteparin-AR
Dalteparin-PL
Pre
Post
pressure(kPa)
Time(min)

Figure 1. A. The flow-pressure waveform of one dog, as an example, with and without in vivo administration of acetylsalicylic acid (ASA). The solid and dotted lines represent before and after ASA administration, respectively. The right-shift of the waveform in the platelet (PL) test indicates delayed occlusion as a result of suppression of platelet aggregation. The waveform for the atheroma (AR) test was essentially unchanged. **B.** The flow-pressure waveform of one dog, as an example, with and without in vitro exposure of blood to dalteparin. The solid and dotted lines represent the before and after dalteparin addition to blood, respectively. The right-shift of the waveform in the AR test indicates delayed occlusion as a result of suppression of coagulation. The waveform for the PL test was essentially unchanged.

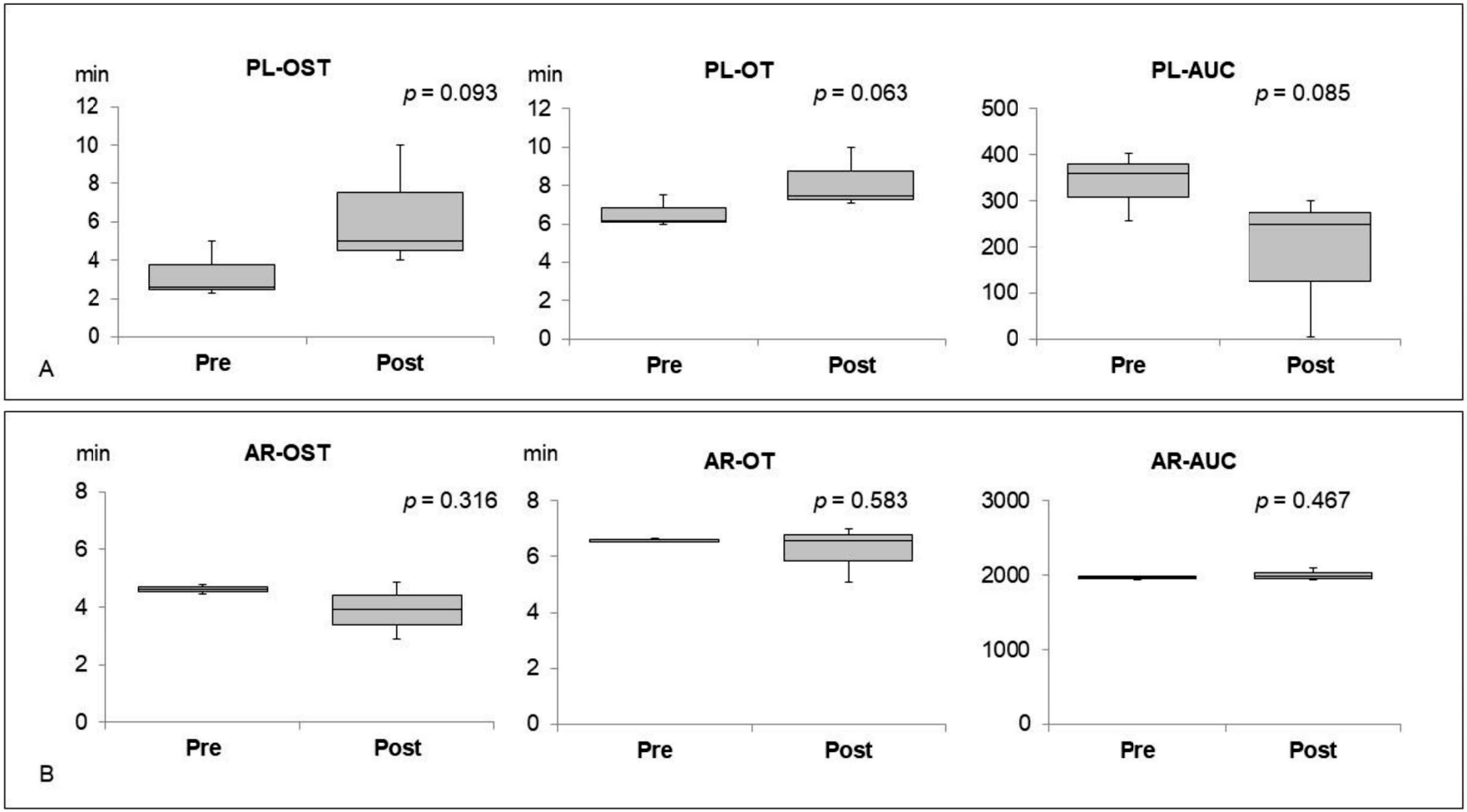
PL-OST
min
p = 0.093
12
10
8
6
4
2
0
Pre
Post
PL-OT
min
p = 0.063
12
10
8
6
4
2
0
Pre
Post
PL-AUC
p = 0.085
500
400
300
200
100
0
Pre
Post
A
AR-OST
min
p = 0.316
8
6
4
2
0
Pre
Post
AR-OT
min
p = 0.583
8
6
4
2
0
Pre
Post
AR-AUC
p = 0.467
3000
2000
1000
0
Pre
Post
B

Figure 2. A. Box-and-whisker plots of the platelet (PL) test before and after administration of acetylsalicylic acid (ASA; n = 3). PL test parameters were not changed significantly by in vivo administration of ASA. **B.** Box-and-whisker plots of the atheroma (AR) test before and after administration of ASA (n = 3). There were no differences in any of these 3 parameters. AUC = area under the pressure curve; OST = occlusion start time; OT = occlusion time.

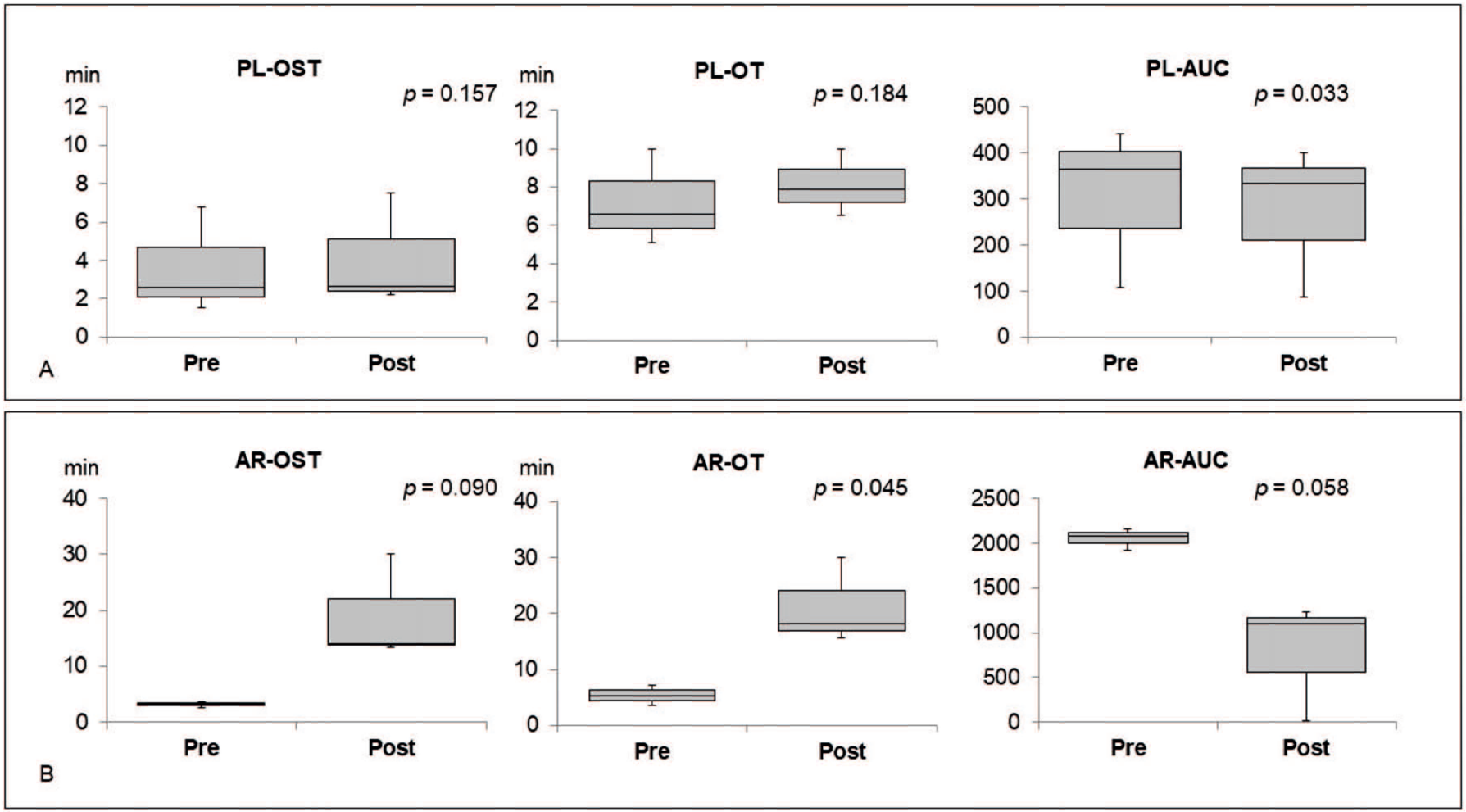
PL-OST
min
p = 0.157
12
10
8
6
4
2
0
Pre
Post
A
PL-OT
min
p = 0.184
12
10
8
6
4
2
0
Pre
Post
PL-AUC
p = 0.033
500
400
300
200
100
0
Pre
Post
AR-OST
min
p = 0.090
40
30
20
10
0
Pre
Post
B
AR-OT
min
p = 0.045
40
30
20
10
0
Pre
Post
AR-AUC
p = 0.058
2500
2000
1500
1000
500
0
Pre
Post

Figure 3. A. Box-and-whisker plots of the platelet (PL) test before and after administration of dalteparin (n = 3). Dalteparin addition did not yield significant changes in occlusion start time (OST) or occlusion time (OT), although the area under the pressure curve (AUC) was altered significantly. **B.** Box-and-whisker plots of the atheroma (AR) test before and after administration of dalteparin (n = 3). AR-OT was changed significantly following in vitro exposure of blood to dalteparin. There was a tendency that AR-OST was prolonged; AR-AUC was decreased

Chapter 3

Assess canine hemostasis with the Total Thrombus-formation Analysis System

1. Abstract

Hemorrhagic diseases are common in dogs. Current coagulation assays do not model all aspects of in vivo hemostasis and may not predict bleeding risk. The Total Thrombus-formation Analysis System (T-TAS) is a novel hemostasis assay system in which whole blood flows through microfluidic channels at defined shear rates to provide qualitative and quantitative evaluation of platelet function (PL-chip) and coagulation function (AR-chip). I evaluated the T-TAS in dogs with hereditary bleeding disorders and with acquired hemorrhagic syndromes (Group 1), and healthy controls (Group 2). Hereditary defects included von Willebrand disease (VWD; n=4), hemophilia A (n=2), and canine Scott syndrome (n=2). Acquired hemorrhagic disorders included neoplastic hemoperitoneum (n=2) and acute hemorrhagic diarrhea syndrome (n=1). Citrate anticoagulated samples were collected from diseased dogs (Group 1, n=11) and controls (Group 2, n=11) for coagulation screening tests, fibrinogen analyses, D-dimer concentration, antithrombin activity, von Willebrand Factor antigen, PFA-100 closure time (PFA-CT) and thromboelastography (TEG). Qualitative thrombus formation in each chip was recorded using the T-TAS video camera. Numeric parameters, derived from the instrument software, included occlusion start time (OST; time to 10kPa), occlusion time (OT; time to 60kPa (PL-chip) or 80kPa (AR-chip)), and area under

the pressure curve (AUC). Correlations between continuous variables were evaluated by Spearman's rank. Continuous variables were compared between groups by Student's t-test or the Mann-Whitney U test. Alpha was set at 0.05. In combined analyses of all dogs, significant correlations were identified between T-TAS variables, between the PFA-CT and PL-chip parameters and between TEG variables and AR-chip parameters. The prothrombin time correlated with the AR-chip AUC at both shear rates. In Group 1 dogs, the AR-chip AUC at low shear was significantly reduced compared with Group 2 dogs. Distinct patterns of aberrant thrombus formation were seen in video images recorded from dogs with VWD and hemophilia A. The T-TAS AR-chip analysis distinguished dogs with bleeding risk compared to healthy controls. Initial evaluations of the T-TAS suggest it may aid characterization of hemostasis in patients at-risk of bleeding and assist with delineating bleeding phenotypes.

2. Introduction

Bleeding disorders are commonly encountered in veterinary medicine[34], and can be challenging to investigate and manage[26]. Hemostasis in vivo occurs through assembly of coagulation factor complexes on the surfaces of activated platelets and tissue factor-bearing cells [2,35]. This cell-based localization of the hemostatic process enables sufficient thrombin to be generated to overcome the effects of dilution by blood flow and the presence of plasma and endothelial anticoagulants.

Although the cell-based model describes the mechanisms of hemostasis in vivo, it is difficult to apply to clinical diagnosis because of the complex interdependence of cellular and plasma factors. Bleeding disorders are typically categorized clinically as defects of platelet number and function (primary hemostasis) or defects of coagulation proteases (secondary hemostasis). Routine tests of hemostasis traditionally evaluate these components in isolation [27]. For instance, primary hemostatic disorders are typically investigated by measuring platelet count, followed by testing the ability of platelets to become activated, to aggregate, to release the contents of their secretory granules and to express a procoagulant surface. Platelet function testing is often performed using isolated platelets, in non-clotting conditions and in the absence of blood flow. Secondary hemostatic

disorders are typically investigated using plasma-based coagulation tests where the endpoint is the time to generate fibrin. Combined evaluation of the prothrombin time (PT) activated partial thromboplastin time (aPTT), and fibrinogen aids in localizing coagulation disorders to the contact pathway, tissue-factor pathway or the common pathway. Specific quantitative and functional factor assays are then used to further define single or combined factor deficiencies or identify the presence of factor inhibitors[27].

Patients with complex hemostatic defects may be difficult to diagnose and manage using these traditional laboratory tests. Test results are often poorly predictive of bleeding risk and do not reflect overall hemostatic balance. Standard tests also ignore the role of erythrocytes in clot formation and stability[36]. The whole blood viscoelastic tests, including thromboelastography (TEG), thromboelastometry (ROTEM) and dynamic viscoelastic coagulometry (Sonoclot) were developed to address some of these shortcomings[5,6], and may aid in predicting bleeding risk[7]. Major limitations of the viscoelastic tests are their insensitivity to platelet function disorders[8,9], and the static nature of the tests that ignores rheology, blood flow and shear effects[10].

The Total Thrombus-formation Analysis System (T-TAS) is a novel microfluidic system that measures whole blood flowing at defined, variable shear rates under

conditions designed to assess platelet function or coagulation and fibrin clot formation[11]. The T-TAS uses whole blood samples that flow through microfluidic chambers coated with collagen and tissue thromboplastin (AR-chip) or collagen only (PL-chip), to focus the evaluation on coagulation or platelet function, respectively [12,13,37]. The system enables quantitative analysis of the timing, extent and rate of thrombus formation and is equipped with a video microscope for real-time imaging and qualitative analyses[14].

In people, the T-TAS system has been used extensively to assess the effects of antithrombotic drugs[12,15], including oral direct Factor Xa inhibitors[16] and antiplatelet agents[17-19]. Studies of patients with coronary artery disease treated with various antithrombotic therapies suggest the T-TAS can predict bleeding risk [20-21]. Consistent with its ability to detect impaired thrombus formation due to antiplatelet drug therapy, the T-TAS system is also sensitive to some inherited platelet function disorders. Patients with platelet storage pool disease (characterized by a reduction in the number or content of alpha granules or dense granules) have decreased thrombus formation in the PL-chip assay, at both low and high shear [14]. In patients with von Willebrand's disease (VWD), the T-TAS appears to be sensitive to moderate to severe plasma von Willebrand factor (VWF) deficiency and the absence of large molecular weight VWF multimers

[22]. Samples from patients with severe type 1 VWD, defined as VWF antigen (VWF:Ag) below 10U/dL, and those with type 2 VWD (absence of large VWF multimers) failed to occlude either AR- or PL-chips but the occlusion times were normal in patients with milder type 1 VWD. In a study of type 1 VWD, patients with relatively prolonged T-TAS PL-chip T10 values had lower VWF levels[23]. Moreover, PL-chip T10 values correlated with bleeding scores and bleeding severity, suggesting that the T-TAS may aid prediction of bleeding risk among patients with type 1 VWD. Published data also suggest the T-TAS can identify hemostatic abnormalities due to coagulation factor deficiencies[24] and essential thrombocythemia [25].

To date, three studies have used the T-TAS to study canine samples. The first evaluated T-TAS reproducibility and established reference intervals in healthy dogs. The PL-chip assay parameters had coefficients of variation (CV) of 6.5-13.6%, while the AR-chip assay parameters had CV values of 1.6-10.0%. This study also assessed the effect of aspirin in 3 dogs and found that the PL-chip assay, but not the AR-chip assay, was affected by antiplatelet therapy [38]. In two related experimental studies of atrial fibrillation induced by rapid atrial pacing, the T-TAS was used to evaluate the propensity of atrial thrombus development [31,32]. The time to initial clot formation (AR-chip T10) of blood collected from the right

atrium and the occlusion time (OT) of both AR- and PL-chips were significantly shorter after 30 minutes of pacing compared to baseline. In contrast, no significant changes were observed in contemporaneous peripheral blood samples [32].

No studies to date have evaluated this system in canine patients with clinical bleeding disorders. The present study therefore aimed to perform T-TAS analyses in parallel with conventional hemostatic testing in dogs with hereditary and acquired bleeding disorders. It was hypothesized that T-TAS measures of platelet-mediated and coagulation-mediated thrombus formation correlate with relevant parameters derived from conventional plasma-based coagulation tests, platelet function analyses, and thromboelastography.

3. Ethics statement

Healthy privately-owned dogs were enrolled as controls with local Institutional Animal Care and Use Committee approval and written informed client consent (Cornell IACUC 2014-0052). Dogs with bleeding disorders were enrolled with local Institutional Animal Care and Use Committee approval and written informed client consent (Cornell IACUC 2014-0053).

4. Material and Method

Animals

Two groups of dogs were recruited for the present study. Criteria for inclusion in Group 1 (dogs with acquired or hereditary bleeding disorders) included hereditary bleeding disorders such as VWD, diagnosed based on genotyping for the presence of a splice site mutation in the VWF gene [39] or deficiency of circulating VWF (VWF:Ag <50% of a canine pooled plasma standard)[40] and Hemophilia A, defined by severe deficiency of coagulation factor VIII (FVIII coagulant activity <10% of canine pooled plasma)[41,42]. Canine Scott syndrome was diagnosed based on abnormal platelet phosphatidylserine externalization and lack of microvesiculation[43]. In addition, dogs with clinical bleeding caused by spontaneous hemoperitoneum or acute hemorrhagic diarrhea syndrome were included in this group. Spontaneous hemoperitoneum was defined as the presence of a hemorrhagic abdominal effusion (packed cell volume greater than 20%) in the absence of trauma, thrombocytopenia, recent antiplatelet agent therapy or known coagulopathy[44]. The diagnosis of acute hemorrhagic diarrhea syndrome was based on the presence of acute onset bloody diarrhea in the absence of underlying disorders such as intestinal parasitism, hypoadrenocorticism, neoplasia or pancreatitis[45]. Group 2 dogs (healthy controls) were eligible for inclusion if they

had no history or evidence of recent or chronic medical conditions, had not received any medication, except for routine preventative healthcare, within the preceding 3 months, and had normal complete blood count and serum biochemistry results. Dogs weighing less than 5kg were excluded to minimize the risk of additional blood sample collection.

Blood sampling and routine clinicopathologic testing

Blood samples were collected by peripheral venipuncture into evacuated tubes using 21g butterfly catheters (Surflo, Terumo, Somerset, NJ). A no-additive tube (BD Vacutainer, BD Biosciences, San Jose, CA) was drawn prior to collection of other samples. These tubes were discarded for dogs in Group 1 and used for serum chemistry testing for Group 2 dogs. For coagulation analyses, PFA-100 closure time (PFA-CT), and thromboelastography, 1.8mL or 2.7mL blood was collected into tubes containing 3.2% sodium citrate in a 1:9 ratio (Vacuette, Greiner Bio-One, Monroe, NC). For T-TAS analyses using AR-chips blood samples were collected into 3.2% citrate, while for T-TAS analyses using PL-chips blood samples were collected into dedicated sample tubes containing hirudin (Hirudin blood tubes, Diapharma, West Chester, OH). Samples for complete blood counts were collected last into K2-EDTA tubes (BD Vacutainer, BD Biosciences, San Jose, CA). Complete

blood cell counts were performed on healthy controls using an ADVIA 2120 (Siemens, Washington, D.C.). Serum chemistry profiles were performed on healthy controls using a Cobas 501 (Roche Diagnostics, Indianapolis, IN). Blood cell counts and biochemical analyses were performed at the institution clinical pathology laboratory.

Coagulation testing and Factor assays

Citrated plasma for clotting time tests and hemostatic protein analyses was prepared by centrifugation of whole blood at 10,000 × g for 10 minutes. The assays were performed at the Comparative Coagulation Laboratory at the Animal Health Diagnostic Center using automated and semi-automated coagulation instruments (STACompact and START4, Diagnostica Stago, Parsippany, NJ). A mechanical endpoint method and human coagulation reagents were used to measure clottable (Clauss) fibrinogen concentration (Fibrinogen, Diagnostica Stago), PT (Thromboplastin LI, Helena Diagnostics, Beaumont, TX) and aPTT (Dade Actin FS, Dade Behring, Newark, DE). Antithrombin (AT) activity was measured with a synthetic chromogenic substrate kit (Stachrom AT III, Diagnostica Stago) and D-dimer concentration was measured in a quantitative, turbidimetric immunoassay (HemosIL D-dimer, Instrumentation Laboratory, Lexington, MA). A

pooled plasma prepared from healthy dogs (n=20) was used as calibration standard for the fibrinogen and AT assays. The fibrinogen content of the plasma standard was determined by gravimetic method[46], and its AT activity was defined as 100%. The D-dimer assay was calibrated with a human D - dimer standard (HemosIL D-dimer calibrator, Instrumentation Laboratory, Bedford, MA). Plasma vWF:Ag was measured in an ELISA configured with monoclonal anti-canine VWF antibodies[47]. Factor VIII coagulant activity (FVIII:C) was measured in a modified aPTT, using a human congenital Factor VIII deficient plasma (George King Biomedical, Overland Park, KS). The standard curves for VWF:Ag and FVIII:C were derived from dilutions of the canine standard which had an assigned value of 100% VWF:Ag and 100% FVIII:C.

Platelet function analyses (PFA-100)

Platelet function under high-shear conditions was evaluated using the PFA - 100 instrument (Siemens HealthCare Diagnostics, Deerfield, IL) according to the manufacturer's instructions. Cartridges containing collagen and ADP as platelet activators (COL/ADP) were used for this study. Citrated whole blood samples were gently mixed and then 800μL was pipetted into the cartridge sample reservoirs for closure time measurement. Assays were performed in duplicate and the mean

value used for subsequent statistical analyses.

Thromboelastography (TEG)

Rotational viscoelastic testing was performed with a computerized instrument (TEG 5000 Hemostasis Analyzer, Haemoscope, Niles, IL) using recalcified, nonactivated - citrated blood (citrate - native) and recalcified - citrated blood activated with recombinant human tissue factor (TF), as previously described [48][49]. Assays were conducted in accordance with the PROVETS guidelines [50][51]. In brief, reaction cups warmed to 37°C were loaded with 20µL of 280mM CaCl2 and either 340µL of citrated blood or 340µL of citrated blood containing a TF - phospholipid reagent (Dade Innovin, Siemens Healthcare Diagnostics, Tarrytown, NY) diluted 1:50,000 in the final (360µL) reaction mixture [49]. The TEG analyses on nonactivated and TF - activated blood were performed simultaneously in 2 channels for 60 - minute run times with compilation of the following TEG parameters: reaction time (R), clotting time (K), angle (α), maximal amplitude (MA), global clot strength (G), and time to maximal rate of thrombus generation (TMRTG) [48].

Thrombin generation (TG)

Banked aliquots of citrate plasma stored at -80°C (for up to 10 months) were used for thrombin generation assays by the calibrated automated thrombogram method. Thrombin generation was measured in an integrated spectrofluorimeter/analytic software instrument (Thrombinoscope, Diagnostica Stago) using the manufacturer's TG reagents (PPP-low, Thrombin calibrator, FLUCa), as previously described [52,53]. Briefly, the assay measures thrombin formation over time in tissue-factor activated, recalcified citrated plasma based on cleavage of a fluorogenic thrombin substrate. Thrombin generation in the test plasma is calculated by comparing fluorescence levels in the tissue factor activated-sample with a paired plasma reaction containing a thrombin calibrator. Coagulation and calibration reactions were performed in triplicate, with 80µL PPP (diluted 1:2 in buffer solution) reacted with either 20µL tissue factor reagent (containing phospholipids and 1 pM human recombinant tissue factor) or 20µL thrombin calibrator. Thrombin generation was monitored for 60 minutes at 10 second intervals in the coagulation and calibrator wells after the addition of 20µL of a solution containing calcium (CaCl2) in HEPES buffer (pH 7.35), and the fluorescent substrate. Reactions were performed in round bottom, high binding polystyrene microtiter plates (Immulon 2HB, Thermo Scientific, Waltham, MA).

Aliquots of canine pooled plasma were included on each test plate as a reagent control. The Thrombinoscope software generates qualitative tracings (thrombograms) and numeric parameters, including the following parameters compiled for statistical analyses: (1) Lag time, defined as the time from assay initiation to the beginning of thrombin generation. (2) Peak, defined as the maximum quantity of thrombin generated during the reaction (nM). (3) Endogenous thrombin potential (ETP), defined by the area under the TG curve and representing the total amount of thrombin formed over 60 minutes.

Evaluation of thrombus formation under flow conditions

Ex vivo thrombus formation was analyzed using the T-TAS instrument (Fujimori Kogyo, Tokyo, Japan) using two types of analysis chips; the PL-chip (channel width 40μm × depth 40μm) (containing 25 capillary channels coated with type-I collagen) and the AR-chip (width 300μm, depth 60μm, length 15mm) (consisting of a single capillary channel coated with collagen and thromboplastin). The PL-chip analyzes platelet-rich thrombus formation under two shear rates (1500s-1, and 2000s-1) and the AR-chip analyzes fibrin-rich thrombus formation under two different shear rates (240s-1 and 600s-1). For PL-chip analysis, 320μL hirudin-anticoagulated whole blood is pipetted into the sample reservoir, then

perfused through the chip at 37°C by a pneumatic pump driving a column of mineral oil. In this assay, platelet activation and thrombus formation are initiated by shear and interactions between platelets and the collagen coating on the capillary channels. For AR-chip analysis, 480μL citrate-anticoagulated whole blood is mixed with 20μL of 0.3M calcium solution containing 1.25mg/mL corn trypsin inhibitor (Fujimori Kogyo, Tokyo, Japan) and immediately pipetted into the reservoir. The recalcified blood is then perfused at 37°C through the AR-chip. During perfusion of blood through the capillary, PLs and the extrinsic coagulation pathway are simultaneously activated through exposure to collagen and tissue thromboplastin. In the AR-chip assay, the effluent blood from the chip is mixed with 25mM EDTA (pH 10.5) solution to prevent occlusion. The process of thrombus formation in both chips is monitored by a pressure sensor located between the pump and the blood sample reservoir that detects flow pressure changes over time. As thrombus formation proceeds on its coated surface, the capillary is gradually occluded, thereby increasing the flow pressure. The following parameters were derived by the instrument's software from T-TAS tracings: (1) OST (occlusion start time or time to reach 10kPa), defined as the time in minutes for the flow pressure to increase from baseline to 10kPa due to partial occlusion of microcapillaries. This parameter defines the onset of thrombus formation. (2) OT (occlusion time),

defined as the time for the flow pressure to reach 60kPa (PL-chip) or 80kPa (AR-chip). This parameter represents the time for complete occlusion of the capillary by thrombus. (3) T10–60 (PL-chip) and T10–80 (AR-chip), defined as the time interval between T10 and OT. This parameter represents the rate of thrombus growth. (4) AUC (area under the curve), defined as the area under the flow pressure curve from baseline to 10 minutes (PL-chip) or from baseline to 30 minutes (AR-chip). This parameter quantifies the amount of thrombus formation during the early part of the reaction if the pressure required to generate an occlusion time is not achieved.

Statistical analysis

Prior to test selection, data were assessed for normality using the D'Agostino Pearson test and descriptive statistics calculated as appropriate. Comparisons of continuous variables between groups were performed using Student's t-tests or the Mann Whitney U test. Associations between continuous variables were evaluated by calculation of Spearman's rank correlation coefficient. Alpha was set at 0.05 and all analyses were conducted using commercial software (JMP 12.2, SAS Institute Inc. and Prism 8.3, GraphPad, La Jolla, CA).

5. Result

Animals

Eleven dogs were enrolled in each group. The bleeding disorder dogs (Group 1) consisted of 8 dogs with hereditary bleeding disorders: 2 Doberman pinschers heterozygous for a VWF mutation and 1 VWF-deficient Doberman (VWD Type 1, n=3), 1 Shetland sheepdog lacking detectable VWF (VWD Type 3), 2 mixed breed dogs with Hemophilia A, and 2 dogs with Scott syndrome (n=1 German shepherd, n=1 Shepherd/Malinois mix). With the exception of acute, severe epistaxis in the Shepherd/Malinois with Scott syndrome, the remaining hereditary defect dogs had no signs of hemorrhage at the time of blood collection. The 3 dogs with acquired defects had active hemorrhage, including 2 mixed breed dogs with neoplastic hemoperitoneum (hemangiosarcoma (n=1), hepatocellular carcinoma and hemangiosarcoma (n=1) and a Boston terrier with acute hemorrhagic diarrhea. The healthy control group dogs (Group 2) included 6 mixed breed dogs, 2 Labrador retrievers, and 1 each of 3 other pure breeds. All Group 2 dogs were deemed clinically healthy based on complete blood counts, serum biochemistry and routine coagulation function testing.

Coagulation testing, VWF:Ag, PFA-100

Results of coagulation tests, VWF:Ag, and PFA100 closure times for Group 1 and Group 2 dogs are displayed in Table 1. As expected, the two dogs with hemophilia A had prolonged aPTT and the two VWF-deficient dogs had maximally prolonged PFA-100 closure times beyond 300 seconds (Table 1). The dog with Scott syndrome and severe epistaxis had slight (0.5 second) prolongation of the aPTT, with marked elevation in fibrinogen and VWF:Ag. Two dogs with hemoperitoneum had marked increases in D-dimer and variably prolonged aPTT, and one had moderate increase in fibrinogen. A single dog in Group 2 had a D-dimer value that was mildly increased compared to the reference interval, but this dog was judged healthy based on physical examination and normal values for all other hemostasis tests (Table 1).

Thrombelastography and Thrombin Generation

Overall, the recalcified only TEG reactions revealed more profound abnormalities in Group 1 dogs than the tissue-factor activated reactions (Figure 2A-C). Both dogs with hemophilia A, and the Scott syndrome dog with acute, severe hemorrhage, had essentially no bonding between the TEG cup and pin in the non-activated reactions, denoted by unmeasurable G (clot strength parameter)

and marked prolongation of R (clot initiation parameter). This failure of clot formation in tissue factor reactions was only consistent for the Scott syndrome dog (Figure 2B, C). The dogs with acquired bleeding disorders had a wide range of TEG abnormalities. Although both dogs with neoplastic hemoperitoneum had prolonged aPTT, one had a high G value and the other a low G value, denoting increased or decreased clot strength relative to values for the controls. Parameters of thrombin generation also differed for these two dogs (Figure 2D, E). The dog with low clot strength also demonstrated relatively low values of peak thrombin formation and thrombin generating potential, suggesting that impaired fibrin formation was due to a failure of coagulation and inadequate fibrinogen cleavage. Two dogs with hemophilia A and one VWF deficient dog also demonstrated low thrombin generation, below that of controls (Figure 2D, E).

T-TAS

Values for the AR-chip AUC at low shear were significantly lower for the Group 1 dogs versus Group 2 controls (P=0.018) (Figure 3). In dogs with VWD (Type 1 and Type 3), the T-TAS video images (Figure 4) suggested that platelet crosslinking was diminished or abnormal. In samples from dogs with Type 1 and Type 3 VWD, thrombus did not readily form perpendicular to the blood flow

direction, thus platelet thrombi rarely spanned the visible gap between the microfluidic channels. In contrast, platelet thrombi did form parallel to the blood flow direction, resulting in accumulation of platelets in front of and adjacent to the microfluidic channel dividers (Data S1, S2). Profiles generated using the AR-chip at a high flow rate from a dog with hemophilia A showed thrombus formation at a normal rate and with normal morphology. In contrast, at low shear, thrombus formation in the dog with hemophilia A was morphologically distinct from normal and caused limited, transient increases in pressure within the flow channel (Figure 5). In one dog with hemoperitoneum and TEG tracings consistent with hypocoagulability (low G values), the AR-AUC at low shear was lower than the mean AR-AUC in healthy dogs (443.5 vs. 1721.2), while the AR-AUC at high shear was closer to the mean AR-AUC healthy dogs (1310.4 vs 1733, respectively). This dog had a normal PT, but mild prolongation of the aPTT (17 sec, with a high normal reference range of 15.5 sec). Results from the PL-chip analysis in this dog were similar to the mean AUC of healthy dogs at both shear levels (medium: 220.9 vs 340 and low: 150.8 vs 275.8, respectively). Of interest, this dog, diagnosed with hepatocellular carcinoma, had a PFA-CT of 187 sec, indicating some decreased platelet function that may have contributed to the low G of the TEG analysis, but which was not reflected in the PL-chip results. The other dog with

hemoperitoneum, despite a mild prolongation of aPTT, had AR- and PL-AUC that were similar to the mean values from the healthy dogs, and had an increased recalcified TEG G value, indicating robust clot strength. A Boston terrier with hemorrhagic diarrhea also had a discordant result between the low shear PL-AUC (61.2 compared to a mean of 275.8 in healthy dogs), and a PFA of 47 sec, representing a normal aperture occlusion time.

Correlations between assays

Calculation of Spearman's rank correlation coefficients between the T-TAS parameters and those generated from the other hemostasis testing identified several statistically significant and biologically plausible associations (Data S2). For the PL-chip (Figure 6), the PFA-CT negatively correlated with the PL-AUC at both low (rs -0.518, P=0.014) and mid shear rates (rs -0.489, P=0.021) and both assay platforms demonstrated failure of thrombus formation in VWF-deficient samples. There were two significant correlations between TG and PL-chip parameters. The PL-AUC at the mid shear rate positively correlated with the ETP (rs 0.562, P=0.008) and with peak thrombin generation (rs 0.440, P=0.046).

For the AR-chip (Figure 7), the PT negatively correlated with the AR-AUC at both the high (rs -0.484, P=0.023) and the low shear (rs -0.489, P=0.021) rates.

There were several significant negative correlations with TEG parameters. The AR-AUC at low shear rate was significantly negatively correlated with the reaction time (R) for the TF activated assay (rs -0.456, P=0.033) and for the recalcified only assay (rs -0.450, P=0.036). There were three significant correlations between TG and AR-chip parameters. The AR-OST at the low shear rate significantly correlated with the ETP parameter (rs -0.648, P=0.002) and the AR-AUC at the low shear rate significantly correlated with the ETP (rs 0.584, P=0.005) and with peak thrombin generation (rs 0.469, P=0.032).

6. Discussion

The T-TAS revealed distinct patterns of aberrant thrombus formation in dogs with defined, hereditary defects of primary and secondary hemostasis. Von Willebrand factor plays a critical role in supporting platelet adhesion to collagen; a property enhanced by VWF conformational changes under flow conditions. As described for human VWD patients, I found that the PL-chip assay was sensitive to VWF deficiency in dogs. In addition to numeric parameters, the T-TAS video-microscopy feature generated dynamic images that clearly demonstrated the consequences of moderate to severe VWF deficiency on platelet thrombus stability. The AR-chip assay includes a thromboplastin coating that triggers coagulation, thus complementing examination of platelet function in the PL-chip. Samples from dogs with hemophilia A demonstrated a delay in clot initiation and weak, non-occlusive clot formation in the AR-chip low shear assay, thus confirming its sensitivity to detect procoagulant factor deficiency in this species. Our preliminary study of dogs with specific defects suggests that combined examination of the T-TAS assays will provide insights into the mechanisms of aberrant thrombus formation in patients with more complex hemostatic disorders.

Analyses of combined results from all dogs revealed correlations between T-TAS parameters and the various traditional tests of the relevant pathway. The PFA-

100 instrument is designed to assess platelet adhesion and aggregate formation under high shear conditions. The inverse association between the PL-chip AUC values and PFA-100 closure time indicates that the unstable platelet thrombi visualized in the T-TAS represent the same phenomenon underlying failure of membrane occlusion and prolongation of PFA-100 closure time. The markedly prolonged closure times and reduced PL-AUC for the two dogs with VWF deficiency are consistent with this critical need for VWF to support platelet adhesion under flow conditions. Flow chamber assays have been instrumental in investigations of the pathogenesis of VWD and of the interactions between VWF and platelet surface receptors [54-57]. I also found a positive correlation between the thrombin generation parameters and the AUC for the PL-chip. Although the hirudin anticoagulant used for PL-chip samples blocks thrombin's ability to form fibrin in the flow chamber, some thrombin-mediated augmentation of platelet aggregation may occur. Stable, occlusive thrombi may form more rapidly, therefore, in samples with higher thrombin generating capacity.

The AR-chip assay initiates coagulation protein complex assembly and activation through contact with thromboplastin under flow conditions. Thus, the AR-chip assay is tuned to identify defects in the onset, propagation, and ultimate stability of fibrin thrombi. Assays focused on one or more of these processes, such

as the prothrombin time and TEG, are therefore likely to demonstrate similar results. Accordingly, I found negative correlations between the AR-chip AUC parameter and clotting time in the PT and the clot reaction time (R-time) in the thromboelastography system. These correlations suggest that delays in forming the initial fibrin strands, representing the assay endpoints of the PT and R-time, are associated with reductions in occlusive thrombus formation under flow conditions. The cleavage of fibrinogen to yield fibrin requires generation of a thrombin burst [3] and correspondingly the AR-chip occlusion start time, and area under the curve parameters were correlated with the endogenous thrombin potential [58]. These associations support the T-TAS's ability to provide further insight into the influence of fluid phase procoagulant protein reactions on platelet and fibrin thrombus formation under flow.

Previous studies in dogs have used flow chamber assays to evaluate platelet interactions with extracellular matrix components[59] and to assess the influence of bacterial infection, lipopolysaccharide and hydroxyethyl starch on platelet function[60]. Flow chamber systems have also been used to study human patients with hemophilia, VWD and hereditary platelet function disorders including May-Hegglin anomaly, gray platelet syndrome, and Glanzmann thrombasthenia[61], all of which are disorders of relevance to canine medicine. The T-TAS has been

used to evaluate healthy dogs and to assess the effects of antiplatelet agents in people [33] and in dogs [38]. In our current study of dogs with bleeding disorders, I found significant differences between healthy and diseased dogs in the AUC parameter only under low shear conditions, suggesting that limiting shear-induced platelet activation may enhance assay sensitivity[62].

As a pilot project, a limitation of the study includes the heterogeneity of the hemostatic defects evaluated. While a breadth of testing was performed in every dog, the total number of dogs was small. Most canine hereditary bleeding disorders are rare, but the present study included dogs with a specific defect of fibrin formation, i.e., hemophilia A, and a specific platelet function defect i.e., VWD. The abnormalities noted in the T-TAS assays recapitulated the underlying mechanism of hemostatic failure for each of these disorders. The platelet defect of Scott syndrome does not impair platelet adhesion or aggregation, and does not influence fibrin formation initiated by an excess of tissue thromboplastin. The traditional and T-TAS assays that monitor these processes showed no abnormalities in the Scott syndrome dog without active hemorrhage. In contrast, the Scott syndrome dog with severe, acute blood loss and epistaxis demonstrated delayed and weak clot formation in the TEG reactions, with corresponding low AUC value in the AR-chip assay. This finding suggests that aberrant ex vivo thrombus formation in the

assay systems was reflective of in vivo hemostatic status. The T-TAS assay has good reproducibility in healthy dogs[38], but the inter-assay variability in disease states is not known and our study did not include serial sampling to evaluate consistency over time, or to evaluate response to therapy. Similarly, it is not known if all of the dogs with the bleeding disorders studied are truly representative of their condition. This is particularly the case with dogs that have acquired bleeding disorders such as those dogs with hemangiosarcoma since the bleeding disorders associated with cancer can be varied and complex[63-65].

In dogs with clinical bleeding, the T-TAS results mirrored those from traditional coagulation testing, with some discrepancies, primarily between the PL-chip and the PFA results. In one case, a prolonged PFA-CT, indicating platelet hypofunction, was not reflected in the PL-chip AUC and in another the opposite occurred. Notably, the PL-chip was tested at low and moderate shear, (1500s-1, and 2000s-1) and not the high shear generated by the PFA (5000s-1)[66]. The combination of both testing modalities may thus be useful to diagnose complex platelet function abnormalities, for instance, as larger vWF molecules may become more important for platelet adhesion at higher shear rates. Another dog had the opposite scenario, with a rapid PFA-CT but lower than expected PL-AUC. This dog had experienced hypovolemic shock and was also experiencing gastrointestinal hemorrhage from

acute hemorrhagic diarrhea syndrome. It is possible that this dog's platelets were activated by the high shear of the PFA, but were in fact hypofunctional at the lower PL-chip shear rates (the moderate shear PL-AUC was similar to healthy dogs).

7. Conclusion

The T-TAS assay detected and characterized primary and secondary hemostatic disorders in dogs. The numeric parameters derived from the T-TAS assays correlated with relevant parameters of other hemostatic tests of similar processes. The T-TAS video-microscopy capabilities also offer novel, qualitative information that complements traditional tests. Use of the two distinct T-TAS assays at different shear rates provides the opportunity for detailed analyses of platelet function disorders and coagulation defects and to incorporate the influence of blood flow into the hemostatic process. Our preliminary results in a limited number of dogs with bleeding disorders suggest that future studies of the T-TAS are warranted. Its unique combination of quantitative and qualitative assessment of thrombus formation will provide mechanistic insights into the pathophysiology of canine hemorrhagic disorders and may prove useful for diagnostic testing, prediction of bleeding severity, and gauging response to therapy.

8. Figures and Table

Abbreviations: aPTT, activated partial thromboplastin time; AT, antithrombin activity; DD, D-dimer; Fg, fibrinogen; Gp, Group; GSD, German shepherd dogs; PFA-CT, Platelet function analyzer-100 closure time; PT, prothrombin time; VWD, von Willebrand's disease; VWF:Ag, von Willebrand factor antigen

Gp	Diagnosis	Breed	Sex	Active bleeding Yes/No	aPTT (s) (8.5-15.5)	PT (s) (11.0-15.5)	Fg (mg/dL) (150-490)	AT (%) (65-145)	DD (ng/mL) (0-575)	VWF:AG (%) (70-180)	PFA-CT (s) (50-120)
1	Type 1 VWD carrier (Genetic test)	Doberman	F	No	12.8	12.8	286	123	217	109	77
	Type 1 VWD carrier (Genetic test)	Doberman	M	No	12.4	13.7	272	118	312	113	100
	Type 1 VWD (VWF deficient)	Doberman	M	No	12.2	13.7	381	118	419	20	>300
	Type 3 VWD (VWF absent)	Shetland sheepdog	FS	No	14.5	13	368	101	413	0	>300
	Hemophilia A	GSD	M	No	26.2	14.2	287	107	83	146	77

	Hemophilia A	GSD	M	No	25.9	14.3	242	111	6	125	73
	Scott syndrome	Mix (GSD x Malinois)	M	Yes	16	13.6	1434	108	63	387	73
	Scott syndrome	GSD	MC	No	11.1	12.5	332	109	191	177	56
	Hemoabdomen, Hemangiosarcoma	Mix	MC	Yes	16.8	11.8	676	80	4511	245	81
	Hemoabdomen, Hepatocellular carcinoma Hemangiosarcoma	Mix	M	Yes	17.5	15	271	110	6051	108	187
	Acute Hemorrhagic Diarrhea Syndrome	Boston terrier	FS	Yes	14.2	13.8	460	75	395	137	47
2	Healthy control	Boxer	FS	No	12.9	12.8	379	93	272	106	99

	Healthy control	Mix	F	No	11.1	12.7	346	103	86	136	87
	Healthy control	Mix	FS	No	14.2	12.5	291	116	92	245	66
	Healthy control	Labrador retriever	FS	No	13.1	12.7	226	105	351	154	62
	Healthy control	Irish wolfhound	FS	No	10.8	12.5	264	109	130	147	57
	Healthy control	Mix	FS	No	10.8	12.1	379	105	459	78	69
	Healthy control	Beagle	MC	No	14.9	11.3	290	125	182	100	92
	Healthy control	Mix	FS	No	11.6	13.2	229	127	270	94	66
	Healthy control	Mix (Mastiff x)	MC	No	13.4	13.3	263	115	788	133	60
	Healthy control	Mix (Labrador x)	FS	No	12.7	13.4	319	115	456	178	50
	Healthy control	Labrador retriever	FS	No	11.1	12.7	368	105	375	102	67

Table 1. Summary of the results of routine coagulation testing for the two groups of dogs analyzed using the T-TAS. Values highlighted in red text were increased above the reference interval. Values highlighted in blue were decreased below the reference interval.

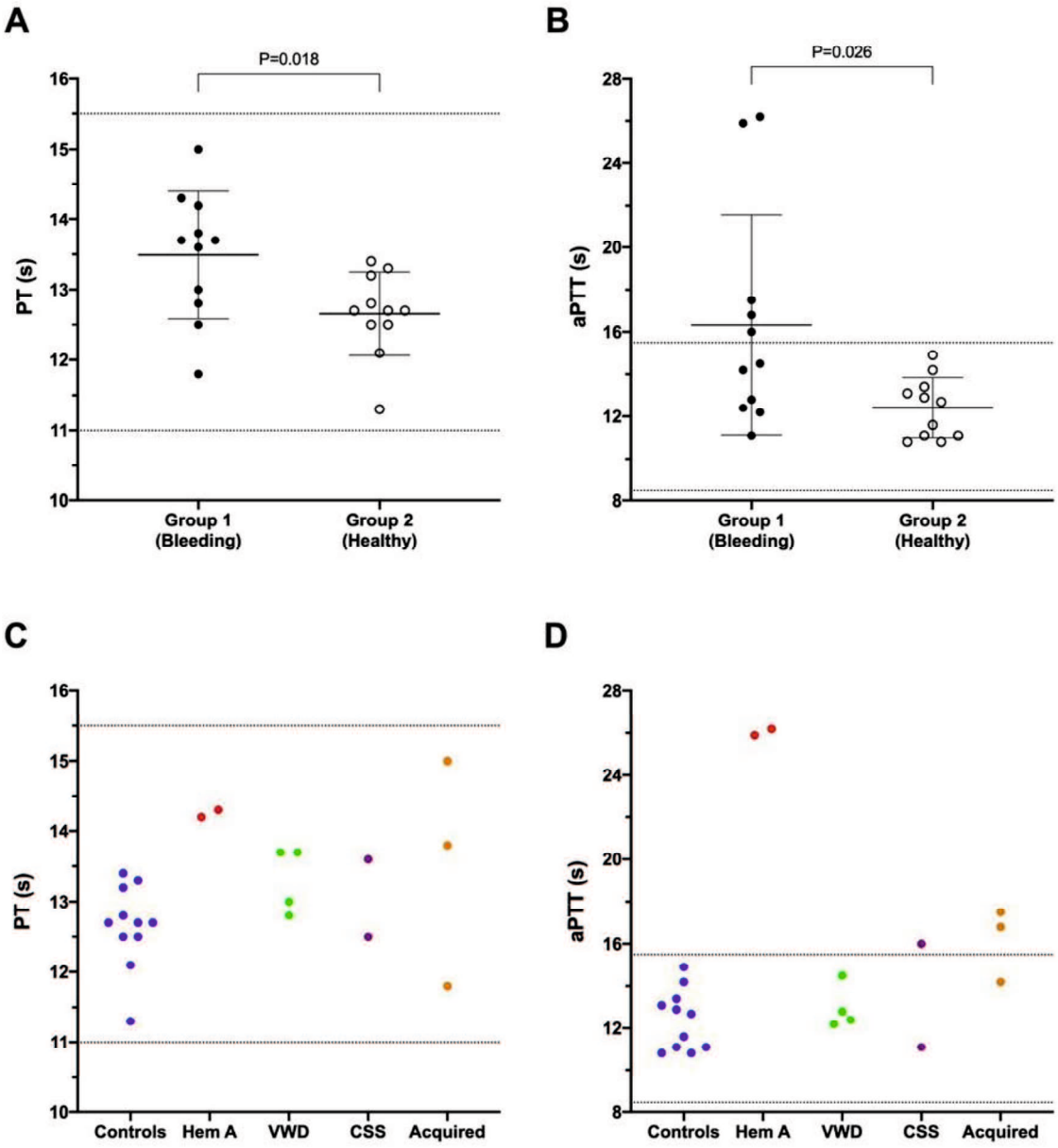
A
P=0.018
PT (s)
16
15
14
13
12
11
10
Group 1
(Bleeding)
Group 2
(Healthy)
B
P=0.026
aPTT (s)
28
24
20
16
12
8
Group 1
(Bleeding)
Group 2
(Healthy)
C
PT (s)
16
15
14
13
12
11
10
Controls
Hem A
VWD
CSS
Acquired
D
aPTT (s)
28
24
20
16
12
8
Controls
Hem A
VWD
CSS
Acquired

Figure 1. Scatterplots comparing the prothrombin time (PT) (A) and activated partial thromboplastin time (aPTT) (B) values of Group 1 (bleeding risk) dogs with those of Group 2 (healthy control) dogs. Values for PT and aPTT in Group 1 were significantly longer than those in Group 2.

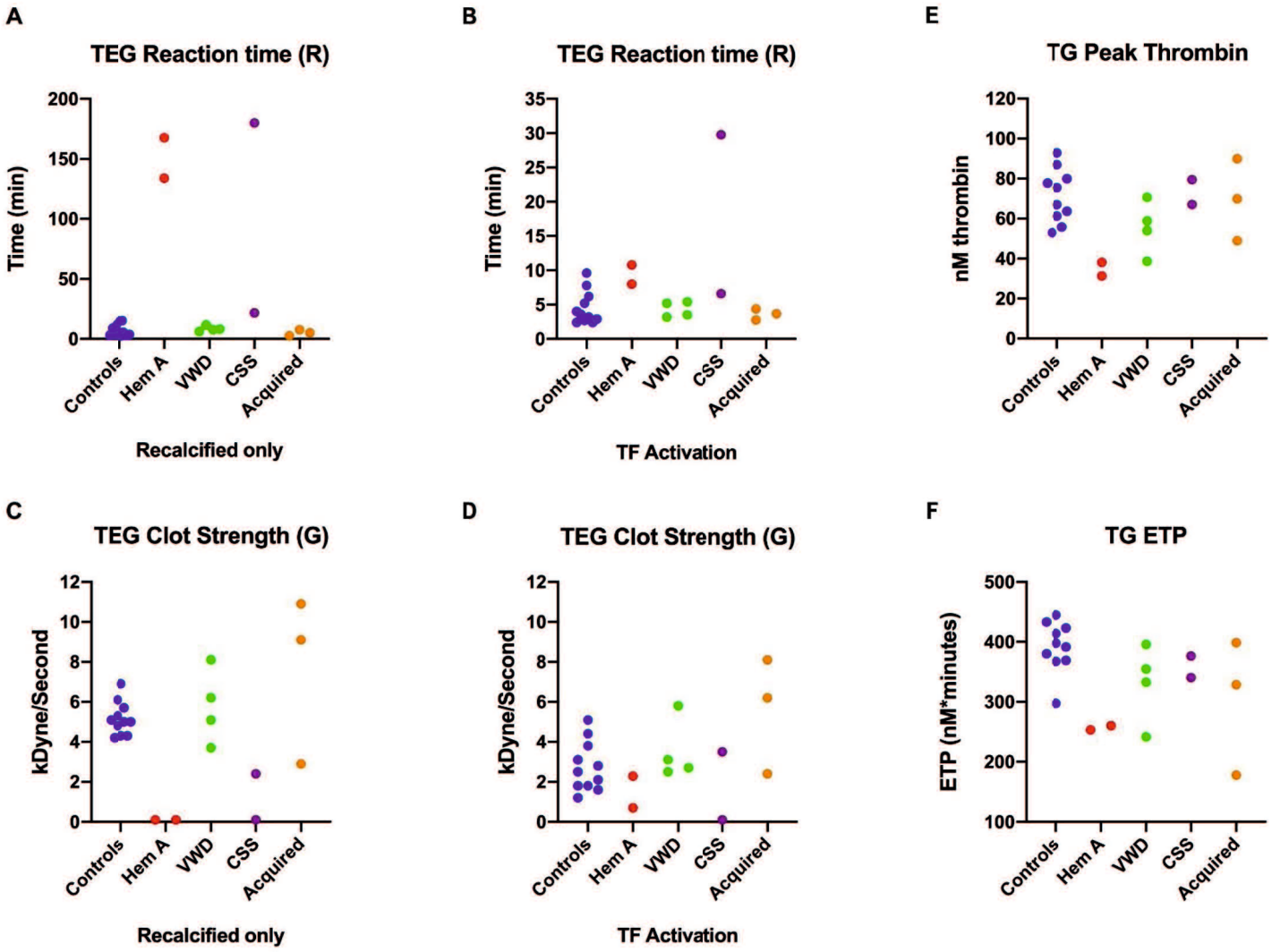
A
TEG Reaction time (R)
Time (min)
200
150
100
50
0
Controls
Hem A
VWD
CSS
Acquired
Recalcified only
B
TEG Reaction time (R)
Time (min)
35
30
25
20
15
10
5
0
Controls
Hem A
VWD
CSS
Acquired
TF Activation
E
TG Peak Thrombin
nM thrombin
120
100
80
60
40
20
0
Controls
Hem A
VWD
CSS
Acquired
C
TEG Clot Strength (G)
kDyne/Second
12
10
8
6
4
2
0
Controls
Hem A
VWD
CSS
Acquired
Recalcified only
D
TEG Clot Strength (G)
kDyne/Second
12
10
8
6
4
2
0
Controls
Hem A
VWD
CSS
Acquired
TF Activation
F
TG ETP
ETP (nM*minutes)
500
400
300
200
100
Controls
Hem A
VWD
CSS
Acquired

Figure 2. Scatterplots comparing key thromboelastography (TEG) and thrombin generation (TG) parameters among dogs in Group 1. (A) Reaction times (R-time) from the citrate recalcified (native) TEG assay. (B) Elastic shear modulus or clot strength values (G) from the citrate recalcified (native) TEG assay. (C) Reaction times from the tissue factor (TF) activated TEG assay. (D) Peak thrombin from the thrombin generation (TG) assay. (E) Endogenous thrombin potential (ETP) derived from the TG assay.

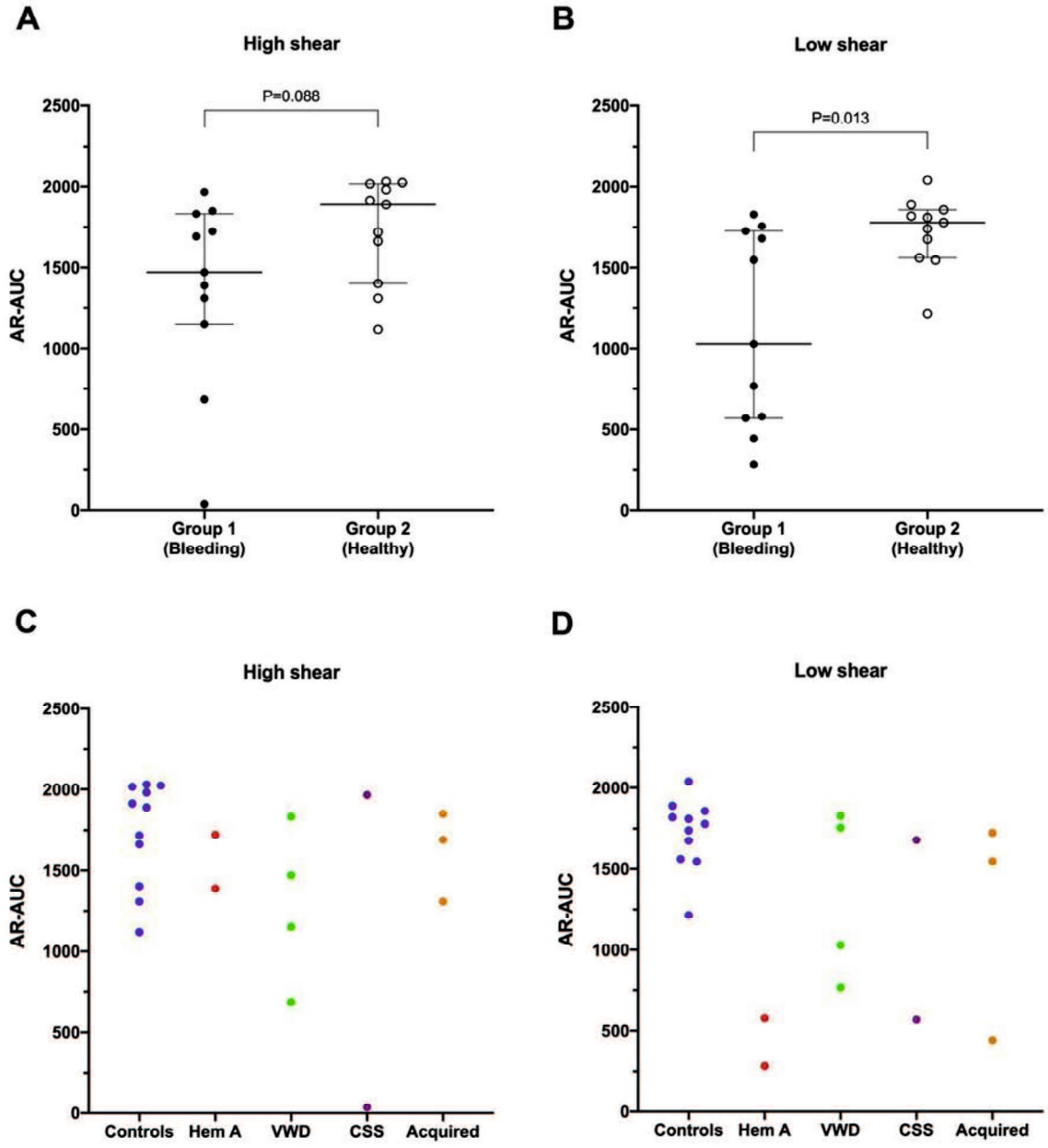
A
High shear
P=0.088
AR-AUC
2500
2000
1500
1000
500
0
Group 1 (Bleeding)
Group 2 (Healthy)
B
Low shear
P=0.013
AR-AUC
Group 1 (Bleeding)
Group 2 (Healthy)
C
High shear
AR-AUC
Controls
Hem A
VWD
CSS
Acquired
D
Low shear
AR-AUC
Controls
Hem A
VWD
CSS
Acquired

Figure 3. The area under the curve value derived from the AR-chip T-TAS assay was not significantly reduced in dogs in Group 1 compared to Group 2 at high shear (A). However, under low shear conditions (B), the area under the curve parameter from the AR-chip assay was significantly reduced in dogs at-risk of bleeding, compared to healthy controls. This suggests the low-shear assay may be more sensitive to the types of bleeding disorders present in the dogs in the study population than is the high-shear assay.

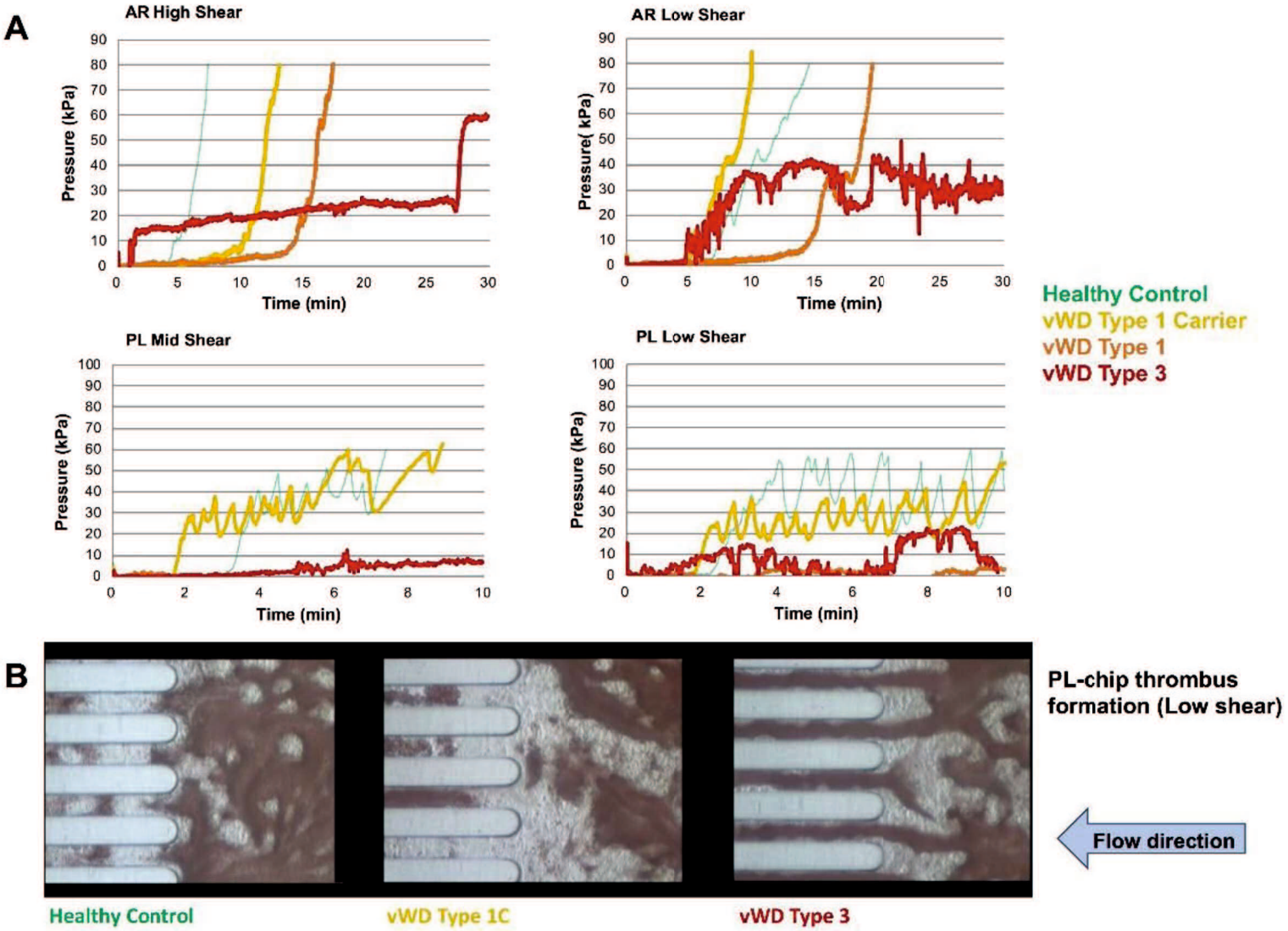
A
AR High Shear
Pressure (kPa)
Time (min)
AR Low Shear
Pressure(kPa)
Time (min)
PL Mid Shear
Pressure (kPa)
Time (min)
PL Low Shear
Pressure (kPa)
Time (min)
Healthy Control
vWD Type 1 Carrier
vWD Type 1
vWD Type 3
B
PL-chip thrombus formation (Low shear)
Flow direction
Healthy Control
vWD Type 1C
vWD Type 3

Figure 4. The T-TAS assay profiles and visualizations of thrombus formation in dogs with von Willebrand's disease (Type 1 carrier, Type 1, Type 3). (A) Pressure-time graphs from AR-chip and PL-chip assays of a healthy control and 3 dogs with vWD. In the AR-chip assays thrombus formation in dogs with type I vWD is delayed (graphs are right-shifted) particularly at high shear, and is incomplete in the dog with type 3 vWD at both high and low shear. The PL-chip profile from the type I vWD carrier dog was similar to that of the healthy control. In the PL-chip assay, the occlusion pressure dog failed to increase in dogs with type 1 or type 3 vWD. (B) Representative images of thrombus formation within the PL-chip microchannels of blood samples from dogs with vWD. In the dog with type 3 vWD, no thrombi can be seen within the PL-chip microchannels.

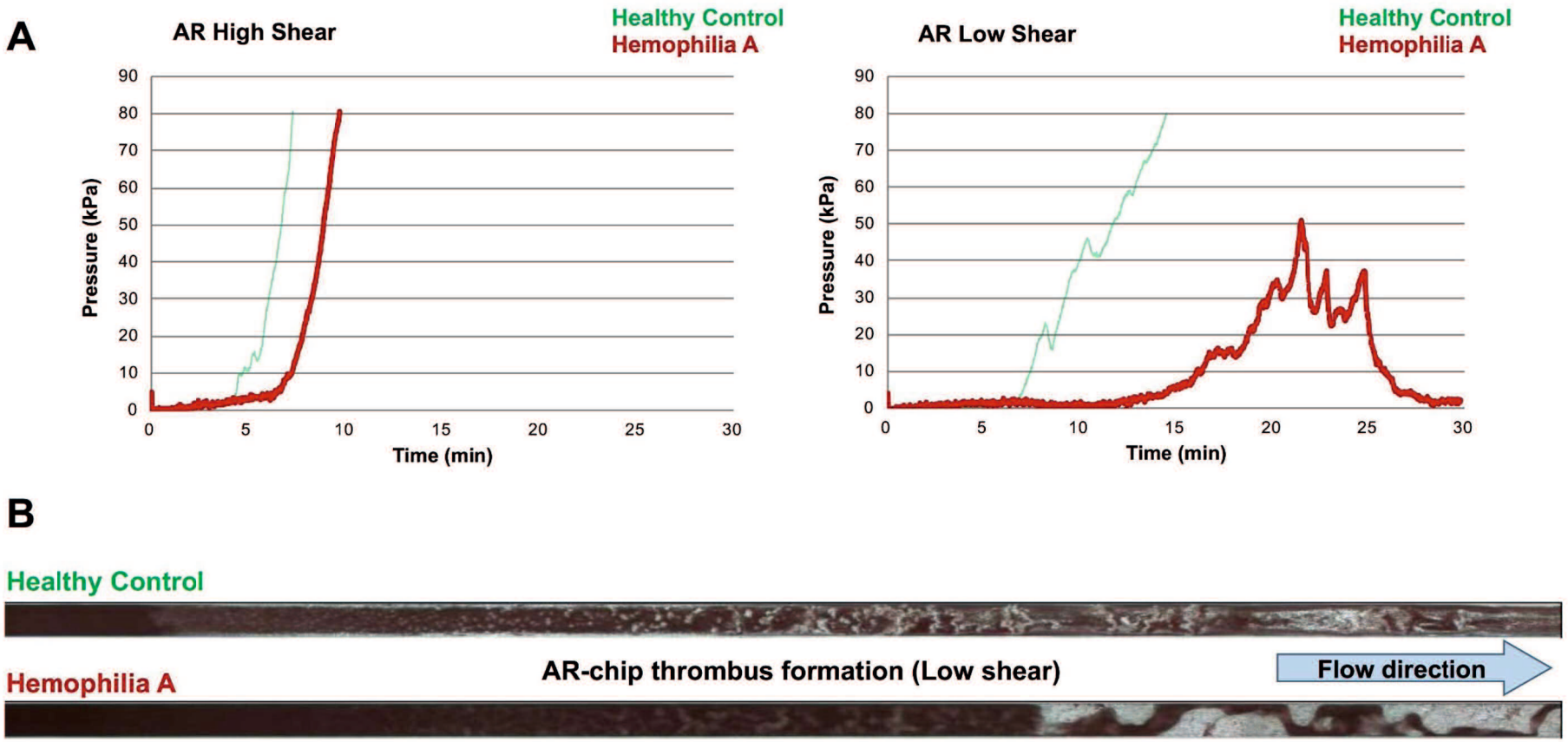
A
AR High Shear
Healthy Control
Hemophilia A
Pressure (kPa)
Time (min)
AR Low Shear
Healthy Control
Hemophilia A
Pressure (kPa)
Time (min)
B
Healthy Control
AR-chip thrombus formation (Low shear)
Flow direction
Hemophilia A

Figure 5. The T-TAS assay profiles and visualizations of thrombus formation in a dog with hemophilia A. (A) At high shear, the AR-chip occlusion profile was normal, while at low shear occlusion was delayed and the profile never reached the endpoint occlusion pressure. (B) In these overview images of the whole AR-chip microchannel the thrombus build-up in the healthy control occurs early and causes complete occlusion. In the dog with hemophilia A, thrombus formation began later in the channel and never became occlusive. An unusual tract can be seen within the thrombus due to ongoing blood flow through and unstable and incomplete blood clot.

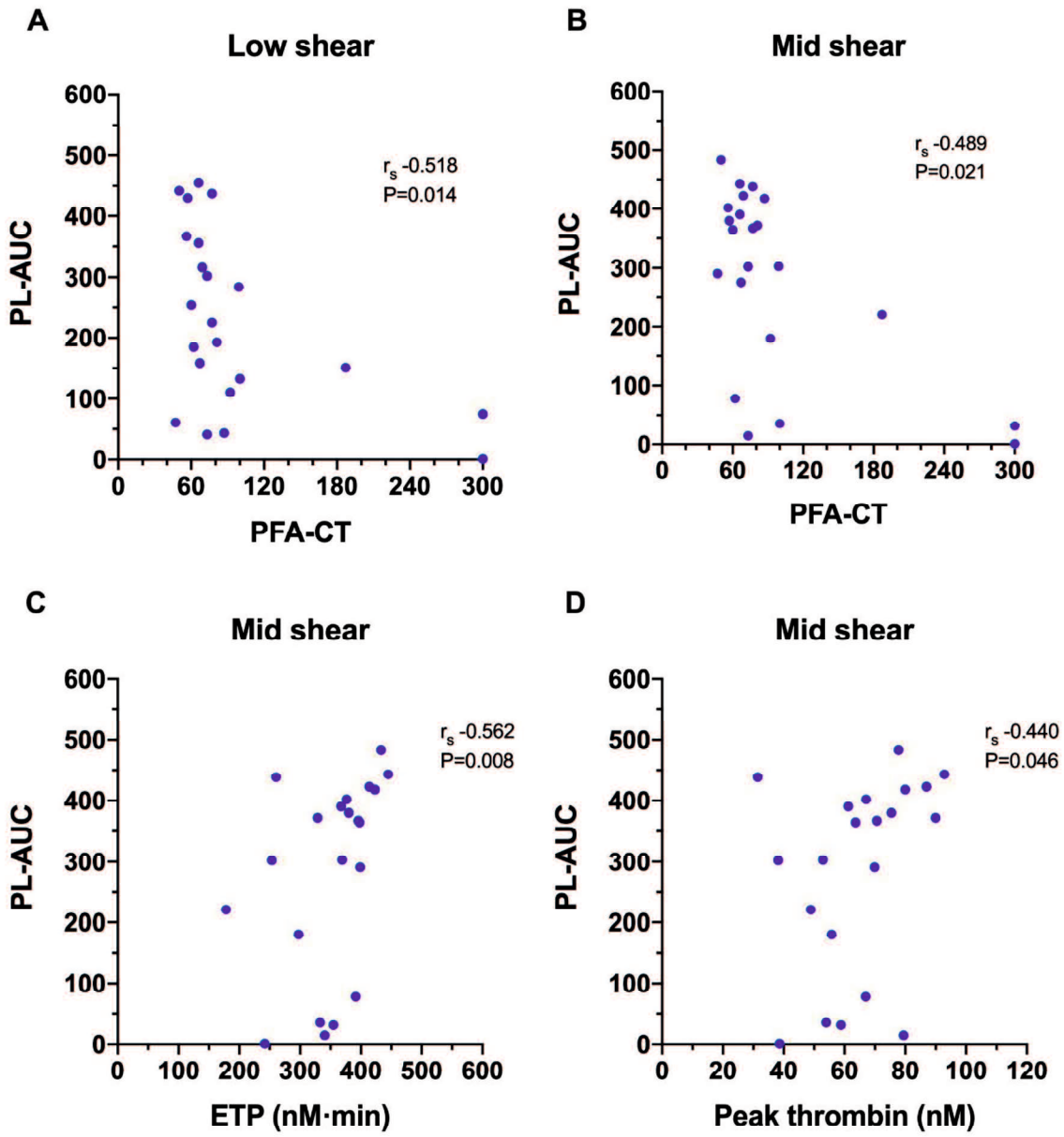
A
Low shear
PL-AUC
PFA-CT
r_s -0.518
P=0.014
B
Mid shear
PL-AUC
PFA-CT
r_s -0.489
P=0.021
C
Mid shear
PL-AUC
ETP (nM·min)
r_s -0.562
P=0.008
D
Mid shear
PL-AUC
Peak thrombin (nM)
r_s -0.440
P=0.046

Figure 6. Scatterplots of T-TAS parameters derived from platelet chip (PL-chip) assays against those derived from routine coagulation tests. (A,B) The closure time of the platelet function analyzer (PFA-CT) was negatively correlated with the PL-chip area under the curve (PL-AUC) at both low and mid-shear suggesting that long closure times are associated with limited platelet thrombus formation under flow conditions. (C, D) The endogenous thrombin potential (ETP) and the peak thrombin generation from the thrombin generation assay were both positively correlated with the area under the curve values from the PL-chip at medium shear (PLM-AUC) suggesting that thrombin generation contributes to thrombus formation in the T-TAS assay under these conditions.

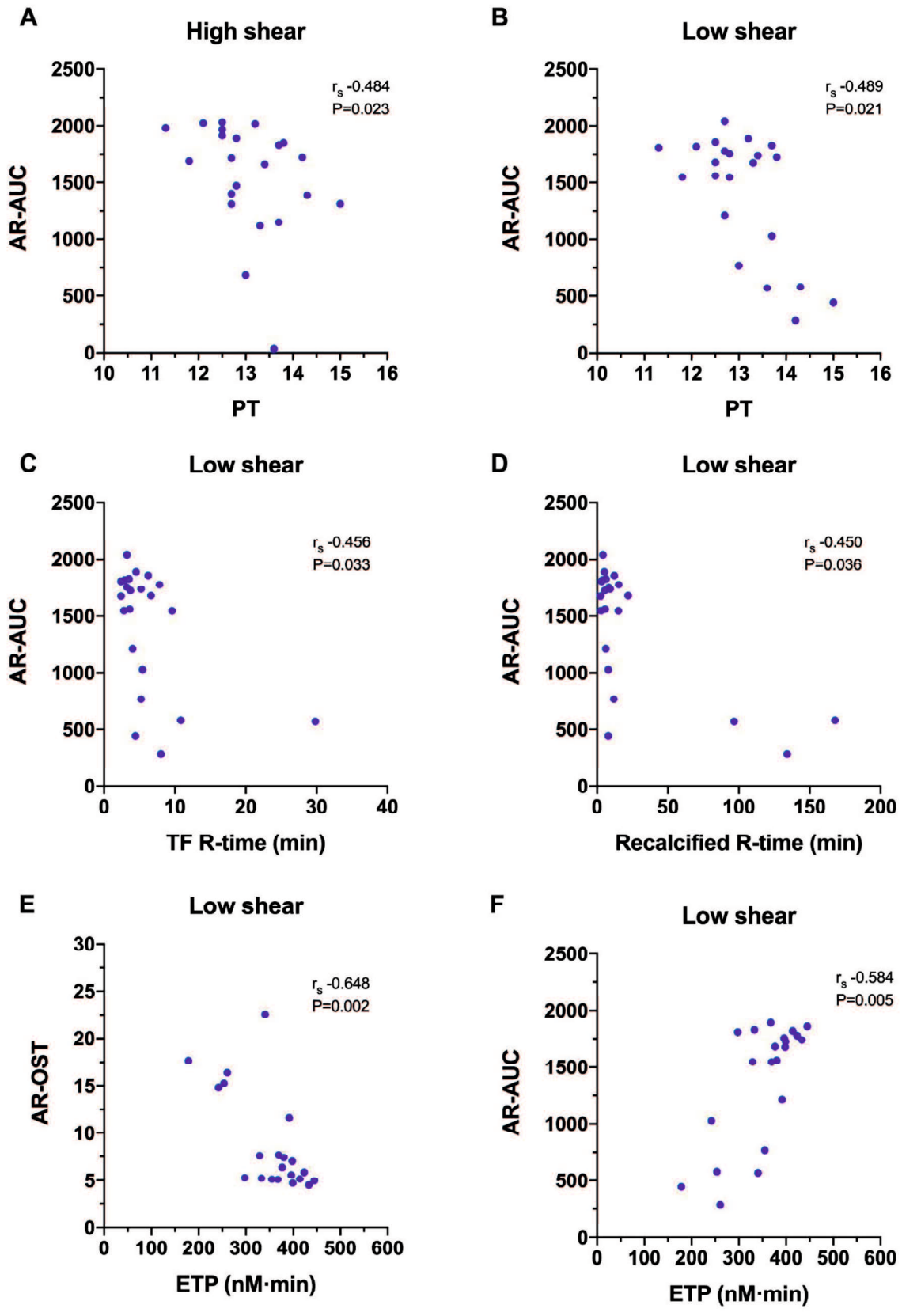
A
High shear
AR-AUC
PT
r_s -0.484
P=0.023
B
Low shear
AR-AUC
PT
r_s -0.489
P=0.021
C
Low shear
AR-AUC
TF R-time (min)
r_s -0.456
P=0.033
D
Low shear
AR-AUC
Recalcified R-time (min)
r_s -0.450
P=0.036
E
Low shear
AR-OST
ETP (nM·min)
r_s -0.648
P=0.002
F
Low shear
AR-AUC
ETP (nM·min)
r_s -0.584
P=0.005

Figure 7. Scatterplots of T-TAS parameters derived atherome chip (AR-chip) assays against those derived from routine coagulation tests. (A, B) The area under the curve (AR-AUC) was negatively correlated with the prothrombin time (PT) at both high and low shear suggesting that long clotting times are associated with reduced extent of thrombus formation under flow conditions. (C, D) The AR-AUC parameter also negatively correlated with the reaction time from the tissue factor and recalcification thromboelastography assays. (E, F) The endogenous thrombin potential (ETG) derived from the thrombin generation assay was negatively correlated with the occlusion start time, and positively correlated with the area under the curve suggesting that the rate and the extent of thrombus formation in the AR-chip assay are related to thrombin generation.

9. Supplementary material

The Supplementary Material for this article can be found online at: https://www.frontiersin.org/articles/10.3389/fvets.2020.00307/full#supplementary-material

Data S1. Representative time-lapse videos of thrombus formation in the platelet-chip (PL-chip) assay in samples from a healthy control dog, two dogs with genetic defects associated with VWD (VWD Type 1c) and two dogs with clinical von Willebrands disease (Type 1 and Type 3). Blood flow was horizontally from right to left. Blood flow was at low shear ($1500s^{-1}$). Videos are 16× normal speed.

Data S2. Representative time-lapse videos of thrombus formation in the platelet-chip (PL-chip) assay in samples from a healthy control dog, two dogs with genetic defects associated with VWD (VWD Type 1c) and two dogs with clinical von Willebrands disease (VWD Type 1 and Type 3). Blood flow was horizontally from right to left. Blood flow was at medium shear ($2000s^{-1}$). Videos are 16× normal speed.

Conclusion

To the best of my knowledge, this thesis project is first investigation for newly developed blood coagulation test, The Total Thrombus-formation Analysis System (T-TAS), in veterinary medicine. The T-TAS, which is a microfluidic assay that simulates conditions in vivo, measures whole blood flow at defined shear rates under conditions designed to assess platelet function (PL-chip) or coagulation and fibrin clot formation (AR-chip). The T-TAS records occlusion start time (OST), occlusion time (OT), and area under the curve (AUC).

In chapter 1, I evaluated the utility of the T-TAS using the healthy control dogs. Based on the results that showed the CVs of all parameters were within under 10%, I conclude the T-TAS would become useful the standard evaluation of canine blood coagulation.

Recently, the veterinary clinicians use several antiplatelet and anticoagulant drugs in dogs. But I had not assessed the effect of these drugs in dogs by the T-TAS. In human medicine, the T-TAS has been used to assess the effect of antiplatelet and anticoagulant drugs. In chapter 2, I confirmed whether each chip of T-TAS can evaluate platelets and coagulation function, respectively. In the study, I investigated the effect of acetylsalicylic acid (ASA) in vivo experiment, and the

effect of an anticoagulation drug (dalteparin; low-molecular-weight heparin; LMWH) in vitro experiment. The inhibition of platelet function by ASA was confirmed by the PL test, and the inhibition of both platelets and coagulation function by LMWH was confirmed by the AR test. The results in chapter 2 suggests that the T-TAS would be useful in the evaluation of canine platelet and blood coagulation function, respectively, and can assess the effect of major antiplatelet and anticoagulant drugs in dogs.

Although hemorrhagic diseases are common in dogs, current coagulation assays do not model all aspects of in vivo hemostasis and, thus, may not predict bleeding risk. In chapter 3, I focused on dogs with hereditary bleeding disorders and with acquired hemorrhagic syndromes to evaluate the T-TAS utility in clinics. Hereditary defects included von Willebrand disease (VWD), hemophilia A, and canine Scott syndrome. Acquired hemorrhagic disorders included neoplastic hemoperitoneum and acute hemorrhagic diarrhea syndrome. In the study, I compared the T-TAS and existing coagulation test including usual coagulation screening tests, fibrinogen analyses, D-dimer concentration, antithrombin activity, von Willebrand Factor antigen, PFA-100 closure time (PFA-CT) and thromboelastography (TEG). As expected, significant correlations were identified between T-TAS variables. PL-chip, which is reflect the platelet function, showed

significant correlation with the PFA-CT and AR-chip, which conducts both platelet and coagulation function, showed significant correlation with TEG variables. These results suggest the correlative utility of the T-TAS to the existing system as a test for hemostasis in dogs. In diseased dogs, the AR-chip AUC at low shear was significantly reduced compared with healthy control dogs. Distinct patterns of aberrant thrombus formation were seen in video images recorded from dogs with VWD and hemophilia A. Thus, the T-TAS AR-chip analysis distinguished dogs with bleeding risk compared to healthy controls. These visual assessments are one of the unique features of the T-TAS and will be more useful tool by accumulating the clinical case as individual diagnosis. These results in chapter 3 strongly suggests that initial evaluations of the T-TAS may aid characterization of hemostasis in patients at-risk of bleeding and assist with delineating bleeding phenotypes.

In closing, my PhD study suggests that the T-TAS has the efficacy to evaluate the platelet and blood coagulation function and valuable as the blood coagulation test in dogs. It is thought that the T-TAS can assess the effect of major antiplatelet and anticoagulant drugs in dogs. The T-TAS can evaluate more correctly the bleeding risks of canine patients in the future by accumulating the clinical samples.

Acknowledgement

I am grateful to Dr. Naoki Miura for all of his supervise, and Dr. Yasuyuki Endo, Dr. Mitsuya Shiraishi, Dr. Masashi Takahashi, and Dr. Kenji Baba for thesis supervision.

I would like to express my sincere gratitude to Dr. Marjory M Brooks, Dr. Robert R Goggs, Dr. Benjamin M Brainard, Dr. Ryuji Fukushima, and Dr. Ikuro Maruyama for their collaboration and helpful supervise this study.

I would like to thank Ms. Tomoka Nagasato and Ms. Ayako Masuda for the help with the examination of samples.

I appreciate Dr. Kazuya Hosokawa and Dr. Tomoko Onishi Wada for advice about the T-TAS machine and support on this study.

I also appreciate Lab members of the Coagulation Laboratory of Cornell University, Emergency Critical Care Unit members of Cornell University, and all staff of Kagoshima University Veterinary Teaching Hospital for many technical bits of help.

I appreciate grateful all animals, patients, and their owners for the cooperation in this study.

Finally, and for most, I would like to especially thank my spouse, Takehiro Iwanaga, for always help to my life.

Appendix

Reference Range

PL										
sample	Base	occlusion start time	occlusion time	⊿ 80- ⊿ 10 time	AUT	RBC	HB	HT	WBC	PLT
G1	3.3	2.683	5.467	2.784	372.9	525.0	12.5	35.4	6000.0	45.6
G1	3.5	2.95	5.433	2.483	362.4	525.0	12.5	35.4	6000.0	45.6
G1	3.6	3.1	5.217	2.117	364.0	548.0	12.4	35.9	4200.0	48.8
G1	3.3	3.867	7.25	3.383	277.7	548.0	12.4	35.9	4200.0	48.8
G1	3.7	3.617	5.567	1.95	342.5	548.0	12.4	35.9	4200.0	48.8
G1	3.3	3.817	6.683	2.866	307.2	548.0	12.4	35.9	4200.0	48.8
G1	4.0	3.117	5.367	2.25	370.6	548.0	12.4	35.9	4200.0	48.8
G1	4.4	3.4	6.2	2.8	320.4	548.0	12.4	35.9	4200.0	48.8
L1	3.8	1.35	3.767	2.417	466.1	500.0	10.6	32.4	7300.0	21.1
L1	3.6	1.433	3.9	2.467	451.2	500.0	10.6	32.4	7300.0	21.1
L1	3.8	1.533	4.233	2.7	428.2	500.0	10.6	32.4	7300.0	21.1
L1	3.2	1.6	4.75	3.15	431.0	502.0	10.1	32.3	7300.0	25.2
L1	3.2	2.167	5.5	3.333	411.0	502.0	10.1	32.3	7300.0	25.2
L1	3.2	2.183	4.933	2.75	416.9	502.0	10.1	32.3	7300.0	25.2
L1	3.1	2.617	6.567	3.95	345.1	502.0	10.1	32.3	7300.0	25.2
L1	3.3	3.017	6.2	3.183	331.0	502.0	10.1	32.3	7300.0	25.2
L1	3.7	1.367	4.65	3.283	415.3	502.0	10.1	32.3	7300.0	25.2

S1	4.0	1.667	3.583	1.916	468.8	813.0	16.3	46.0	9900.0	23.9
S1	4.1	1.933	4.15	2.217	432.6	813.0	16.3	46.0	9900.0	23.9
T1	4.5	2.417	3.967	1.55	431.4	875.0	18.2	54.2	12000.0	30.5
T1	4.2	2.067	3.35	1.283	455.9	875.0	18.2	54.2	12000.0	30.5
T1	4.5	2.517	3.35	0.833	440.0	875.0	18.2	54.2	12000.0	30.5
T1	5.0	1.65	3.5	1.85	463.8	875.0	18.2	54.2	12000.0	30.5
G2	3.5	2.767	5.167	2.4	370.0	525.0	12.5	35.4	6000.0	45.6
G2	3.5	2.367	3.867	1.5	430.0	525.0	12.5	35.4	6000.0	45.6
G2	5.9	0.9	3.717	2.817	473.3	525.0	12.5	35.4	6000.0	45.6
L2	5.2	1	3.567	2.567	476.0	500.0	10.6	32.4	7300.0	21.1
L2	3.9	1.083	2.55	1.467	493.6	500.0	10.6	32.4	7300.0	21.1
L2	4.7	1.25	6.817	5.567	362.7	500.0	10.6	32.4	7300.0	21.1
S2	4.2	2.383	3.017	0.634	450.0	813.0	16.3	46.0	9900.0	23.9
S2	3.6	2.4	4.9	2.5	408.9	813.0	16.3	46.0	9900.0	23.9
S2	4.0	1.983	3.3	1.317	455.4	813.0	16.3	46.0	9900.0	23.9
S2	3.6	2.45	5.467	3.017	397.4	813.0	16.3	46.0	9900.0	23.9

AR										
sample	Base	occlusion start time	occlusion time	⊿80-⊿10 time	AUT	RBC	HB	HT	WBC	PLT
L	3	3.417	4.433	1.016	2092.9	523	10.8	32.2	5800	15.8
	2.9	4.267	5.117	0.850	2034.7	523	10.8	32.2	5800	15.8
		3.750	5.250	1.500	2035.0	523	10.8	32.2	5800	15.8
G	2.8	3.433	4.883	1.450	2066.6	459	10.8	29.3	3800	28.2
	2.8	3.533	4.967	1.434	2069.5	459	10.8	29.3	3800	28.2
	2.7	4.650	6.017	1.367	1990.5	459	10.8	29.3	3800	28.2
	2.8	3.983	4.883	0.900	2063.0	459	10.8	29.3	3800	28.2
S	3	3.517	4.617	1.100	2084.2	646	12.8	36.6	9400	23.4
	3	3.950	5.400	1.450	2043.2	646	12.8	36.6	9400	23.4
	3	4.083	5.017	0.934	2046.8	646	12.8	36.6	9400	23.4
B1	3	4.583	6.033	1.45	1993.0	672	14.9	43.9	7700	21.5
	2.9	5.500	7.017	1.52	1906.8	672	14.9	43.9	7700	21.5
	2.9	6.383	8.350	1.97	1832.4	672	14.9	43.9	7700	21.5
B2	3.2	9.267	10.933	1.666	1607.0	579	13.6	40.3	8900	30.4
	3.1	8.167	10.633	2.466	1667.7	579	13.6	40.3	8900	30.4
	3.1	8.217	10.033	1.816	1679.6	579	13.6	40.3	8900	30.4
B3	3.1	5.200	6.633	1.433	1947.5	662	14.7	40.5	7900	31.9
	3.2	4.450	5.483	1.033	2010.6	662	14.7	40.5	7900	31.9
	3.1	4.950	5.900	0.950	1980.7	662	14.7	40.5	7900	31.9

Healthy Control for CV

PL									
sample	occlusion start time	occlusion time	⊿ 80- ⊿ 10 time	AUT	RBC	HB	HT	WBC	PLT
G	2.683	5.467	2.784	372.9	525.0	12.5	35.4	6000.0	45.6
	2.95	5.433	2.483	362.4					
	2.767	5.167	2.4	370.0					
	2.367	3.867	1.5	430.0					
	0.9	3.717	2.817	473.3					
G	2.85	3.383	0.533	424.8	548.0	12.4	35.9	4200.0	48.8
	3.1	5.217	2.117	364.0					
	3.867	7.25	3.383	277.7					
	3.617	5.567	1.95	342.5					
	3.817	6.683	2.866	307.2					
	3.117	5.367	2.25	370.6					
	3.4	6.2	2.8	320.4					
L	1.35	3.767	2.417	466.1	500.0	10.6	32.4	7300.0	21.1
	1.433	3.9	2.467	451.2					
	1.533	4.233	2.7	428.2					
	1	3.567	2.567	476.0					
	1.083	2.55	1.467	493.6					
	1.25	6.817	5.567	362.7					

L	1.6	4.75	3.15	431.0	502.0	10.1	32.3	7300.0	25.2
	2.167	5.5	3.333	411.0					
	2.183	4.933	2.75	416.9					
	2.617	6.567	3.95	345.1					
	3.017	6.2	3.183	331.0					
	1.367	4.65	3.283	415.3					
S	1.667	3.583	1.916	468.8	813.0	16.3	46.0	9900.0	23.9
	1.933	4.15	2.217	432.6					
	2.383	3.017	0.634	450.0					
	2.4	4.9	2.5	408.9					
	1.983	3.3	1.317	455.4					
	2.45	5.467	3.017	397.4					
T	2.267	4	1.733	442.2	875.0	18.2	54.2	12000.0	30.5
	2.35	3.117	0.767	450.0					
	2.417	3.967	1.55	431.4					
	2.067	3.35	1.283	455.9					
	2.517	3.35	0.833	440.0					
	1.65	3.5	1.85	463.8					
B1	1.967	5.367	3.400	432.3	635.0	14.2	41.1	8900.0	19.0
	2.033	5.817	3.784	392.0					
B1	2.15	6.617	4.467	378.4	672.0	14.9	43.9	7700.0	21.5
	2.15	7.717	5.567	333.1					
	2.583	6.867	4.284	330.4					
	2.25	7.433	5.183	338.1					

B2	3.667	4.633	0.966	365.0	651.0	15.7	43.4	8300.0	27.9
	2.9	5.867	2.967	353.2					
	3.867	6.233	2.366	329.7					
	4.817	6.783	1.966	269.3					
B2	2.833	6.117	3.284	366.3					
	2.983	4.717	1.734	389.5					
	2.9	4.117	1.217	404.9					
	2.867	4.067	1.2	410.2					
B3	3.000	5.333	2.333	381.4	846.0	18.0	53.3	9400.0	39.5
	2.867	6.65	3.783	350.5					
B3	2.633	5.333	2.7	377.6	810.0	17.8	51.0	9800.0	28.5
	2.617	4.85	2.233	392.7					
	2.683	4.217	1.534	413.7					
	2.6	4.667	2.067	405.2					
AR									
sample	occlusion start time	occlusion time	⊿80-⊿10 time	AUT	RBC	HB	HT	WBC	PLT
L	3.417	4.433	1.016	2092.9	523	10.8	32.2	5800	15.8
	4.267	5.117	0.850	2034.7					
	3.750	5.250	1.500	2035.0					
L	3.017	4.3	1.283	2112.4	501	10.1	31.4	4600	14.2
	3.200	4.483	1.283	2103.4					
	2.867	4.117	1.25	2126.8					
G	3.433	4.883	1.450	2066.6	459	10.8	29.3	3800	28.2

	3.533	4.967	1.434	2069.5					
	4.650	6.017	1.367	1990.5					
	3.983	4.883	0.900	2063.0					
G	2.900	4.017	1.117	2133.9	486	11.4	31.2	4200	41.8
	2.767	4.117	1.350	2129.1					
	2.917	4.367	1.450	2121.9					
S	3.517	4.617	1.100	2084.2	646	12.8	36.6	9400	23.4
	3.950	5.400	1.450	2043.2					
	4.083	5.017	0.934	2046.8					
S	3.117	4.600	1.483	2113.1	723	14.1	41.9	8800	24.1
	3.167	4.533	1.366	2097.5					
	3.750	4.967	1.217	2057.8					
S	3.283	4.917	1.634	2085.7	692	13.5	33.2	9400	26.5
	2.833	4.083	1.250	2130.4					
	3.850	5.417	1.567	2052.1					
B1	3.883	5.65	1.767	2029.0	635.0	14.2	41.1	8900.0	19.0
	3.483	5.7	2.217	2021.3					
B1	4.583	6.0	1.45	1993	672	14.9	43.9	7700	21.5
	5.5	7.0	1.517	1906.8					
	6.383	8.4	1.967	1832.4					
B2	3.767	5.45	1.683	2039.2	651.0	15.7	43.4	8300.0	27.9
	4.433	6.2	1.767	1991.2					
B2	9.267	10.9	1.666	1607	579	13.6	40.3	8900	30.4
	8.167	10.6	2.466	1667.7					

	8.217	10.0	1.816	1679.6					
B3	3.95	5.383	1.433	2040.8	846.0	18.0	53.3	9400.0	39.5
	4.683	5.733	1.05	1993.0					
B3	5.2	6.633	1.433	1947.5	662	14.7	40.5	7900	31.9
	4.45	5.488	1.038	2010.6					
	4.95	5.9	0.95	1980.7					

Aspirin Data

	OST	OT	OT-OST	AUC
PL Pre	2.3	5.95	3.65	402.8
PL Pre	4.967	7.517	2.55	256.8
PL Pre	2.583	6.183	3.6	359
PL 2H	4.017	7.083	3.066	299.2
PL 2H	3.15	6.367	3.217	334.8
PL 2H	10	10	0	7
PL 2H	9.117	10	0.883	29.8
PL 2H	5.017	7.45	2.433	248.4
PL 2H	3.417	5.9	2.483	347.5
PL 6H	2.883	9.333	6.45	284.6
PL 6H	2.867	10	7.133	222.6
PL 6H	10	10	0	4
PL 6H	6.733	10	3.267	91.8
PL 6H	4.65	5.683	1.033	305.4
PL 6H	5.8	8.5	2.7	91.8

	OST	OT	OT-OST	AUC
AR Pre	4.45	6.667	2.217	1962.3
AR Pre	4.633	6.533	1.9	1961.6
AR Pre	4.767	6.533	1.766	1961.3
AR 2H	3.933	6.567	2.634	1983.4
AR 2H	3.85	5.55	1.7	2039
AR 2H	2.867	5.083	2.216	2095.8
AR 2H	3.483	5.433	1.95	2055.7
AR 2H	4.867	6.983	2.116	1934
AR 2H	4	5.617	1.617	2036.8
AR 6H	5.933	8.333	2.4	1835.3
AR 6H	4.167	6.4	2.233	1987.9
AR 6H	3.133	5.083	1.95	2075.4
AR 6H	3.517	5.817	2.3	2039.8
AR 6H	5.25	7.3	2.05	1906.8
AR 6H	4.45	6.117	1.667	1994.3

Low Molecular Weight Heparin Data

		10.0(kPa)	20.0(kPa)	30.0(kPa)	40.0(kPa)	50.0(kPa)	60.0(kPa)	70.0(kPa)	80.0(kPa)	AUC	OT-OST
Dog 1	PL12	2.6	2.683	2.767	2.9	3.967	6.55			364	3.95
	PL12+Heparin	2.65	2.75	2.833	3	6.783	7.867			332.9	5.217
	AR10	3.233	3.6	3.9	4.083	4.233	4.883	5.117	5.3	2075.5	1.65
	AR10+Heparin	14.1	15.35	15.733	15.85	16.45	16.6	18	18.067	1105.6	2.5
Dog 2	PL12	1.55	1.633	1.683	2.183	3.233	5.067			441	3.517
	PL12+Heparin	2.2	2.25	2.317	2.383	3.067	6.517			401.2	4.317
	AR10	2.65	2.783	2.9	3.117	3.25	3.35	3.45	3.533	2161.5	0.7
	AR10+Heparin	13.45	14.25	14.717	14.983	15.133	15.317	15.467	15.567	1236.1	1.867
Dog 3	PL12	6.783	7.3	7.6	7.883	8.65	0			108.3	
	PL12+Heparin	7.517	8.017	8.367	9.283	9.95	0			88.1	
	AR10	3.683	5.967	6.333	6.783	6.9	6.983	7.05	7.117	1918.3	3.434
	AR10+Heparin	0	0	0	0	0	0	0	0	18.9	

Healthy Control Data

PL-Mid	Sequence#	Date	Breed	Sex	Status	10.0 (kPa)	20.0 (kPa)	30.0 (kPa)	40.0 (kPa)	50.0 (kPa)	60.0 (kPa)	AUC
	1	10/4/2018	Boxer	S	Healthy/control	3.633	3.750	4.000	4.200	6.033	7.650	302.9
	3	10/9/18	Mix	F	Healthy/control	2.233	2.300	2.433	2.667	2.833	5.367	418.2
	5	10/18/18	Mix	S	Healthy/control	1.883	2.083	2.217	2.367	4.167	4.333	443.2
	8	10/26/18	Labrador R	S	Healthy/control	8.550	8.933	9.233	9.400	9.600	9.833	78.0
	9	11/02/2018	Irish Wolfhound	S	Healthy/control	2.083	2.183	2.317	2.467	2.8	6.633	380.2
	10	11/8/2018	Mix	S	Healthy/control	2.417	2.65	2.733	3.017	3.683	4.117	422.7
	11	11/9/2018	Beagle	C	Healthy/control	5.633	6.167	7.117	7.867	8.567	8.65	180.2
	12	11/9/2018	Mix	S	Healthy/control	2.183	2.317	3.483	4.583	4.7	4.967	390.5
	14	11/19/2018	Mix (Mastiff?)	C	Healthy/control	2.283	2.367	2.517	2.7	6.417	6.567	364.9
	15	11/20/2018	Lab x Mastif susp	S	Healthy/control	1.65	1.7	1.783	1.867	1.967	2.883	483.6
	16	11/21/2018	Labrador R	S	Healthy/control	2.983	3.3	3.467	4.25	6.417	0	276.3

PL-Low	1	10/4/2018	Boxer	S	Healthy/control	2.733	3	3.333	3.917	4.217	0	284.3
	3	10/9/18	Mix	F	Healthy/control	8.883	9.167	9.35	9.683	0	0	43.5
	5	10/18/18	Mix	S	Healthy/control	2.1	2.2	2.333	2.467	2.683	3.333	455.0
	8	10/26/18	Labrador R	S	Healthy/control	0.617	5.417	5.900	7.033	7.117	0.000	184.6
	9	11/02/2018	Irish Wolfhound	S	Healthy/control	2.25	2.483	2.633	2.817	3.3	4.133	430
	10	11/8/2018	Mix	S	Healthy/control	3.233	3.483	3.75	3.883	4.517	7.717	315.8
	11	11/9/2018	Beagle	C	Healthy/control	6.85	7.267	7.6	8.85	9.883	0	110.5
	12	11/9/2018	Mix	S	Healthy/control	1.717	1.8	1.967	3.117	6.467	6.633	355.7
	14	11/19/2018	Mix (Mastiff?)	C	Healthy/control	2.167	2.283	2.5	2.95	9.8	0	254
	15	11/20/2018	Lab x Mastif susp	S	Healthy/control	2.617	2.717	2.8	2.867	2.95	3	442.1
	16	11/21/2018	Labrador R	S	Healthy/control	7.067	7.333	7.433	7.517	7.85	8.3	158.6

AR-High	Sequence#	Date	Breed	Sex	Status	10.0 (kPa)	20.0 (kPa)	30.0 (kPa)	40.0 (kPa)	50.0 (kPa)	60.0 (kPa)	70.0 (kPa)	80.0 (kPa)	AUC
	1	10/04/2018	Boxer	S	Healthy/control	4.917	6.050	6.317	6.700	6.983	7.200	7.433	7.550	1890.4
	3	10/09/2018	Mix	F	Healthy/control	12.150	13.017	13.250	14.133	14.483	14.700	14.850	14.983	1309.4
	5	10/18/2018	Mix	S	Healthy/control	4.150	4.500	4.667	4.817	4.967	5.067	5.150	5.200	2031.4
	8	10/26/2018	Labrador R	S	Healthy/control	6.850	7.850	8.400	8.950	9.450	9.733	9.950	10.133	1717.5
	9	11/02/2018	Irish Wolfhound	S	Healthy/control	4.95	5.083	5.2	5.833	6.817	6.967	7.117	7.25	1914.5
	10	11/08/2018	Mix	S	Healthy/control	3.733	4.4	4.5	4.617	5.217	5.433	5.583	5.767	2024.9
	11	11/0	Beagl	C	Health	4.017	4.833	5.217	5.583	5.883	6.083	6.25	6.467	1981

		9/20 18	e		y/contr ol									
	12	11/0 9/20 18	Mix	S	Health y/contr ol	3.983	4.35	4.7	4.933	5.183	5.467	5.633	5.75	2017.3
	14	11/1 9/20 18	Mix (Mast iff?)	C	Health y/contr ol	15.283	15.833	16.117	16.283	16.4	16.617	16.733	16.833	1118.9
	15	11/2 0/20 18	Lab x Masti f susp	S	Health y/contr ol	8.9	9.333	9.583	9.733	9.967	10.1	10.183	10.333	1662.9
	16	11/2 1/20 18	Labra dor R	S	Health y/contr ol	11.8	12.2	12.55	12.75	12.933	13.033	13.15	13.25	1402.2
AR-Low	1	10/0 4/20 18	Boxer	S	Health y/contr ol	7.667	8.317	9.517	10.250	12.000	13.100	14.050	14.750	1546.3
	3	10/0 9/20 18	Mix	F	Health y/contr ol	5.883	6.900	7.533	7.867	8.517	8.900	9.167	10.050	1779.1
	5	10/1 8/20 18	Mix	S	Health y/contr ol	4.983	6.000	6.350	6.900	7.783	7.967	8.083	8.217	1858.1

	8	10/26/2018	Labrador R	S	Healthy/control	11.633	14.017	15.083	15.650	16.167	16.750	17.283	17.683	1214.8
	9	11/02/2018	Irish Wolfhound	S	Healthy/control	7.417	7.783	8.117	9.283	9.917	13.383	13.8	14.183	1560.6
	10	11/08/2018	Mix	S	Healthy/control	5.15	5.617	6.017	7.9	8.467	8.917	9.217	9.45	1818.9
	11	11/09/2018	Beagle	C	Healthy/control	5.267	5.9	6.65	7.933	8.55	8.983	9.467	9.867	1809.3
	12	11/09/2018	Mix	S	Healthy/control	5.1	5.533	5.883	6.15	7.033	7.65	8.083	8.583	1890.2
	14	11/19/2018	Mix (Mastiff?)	C	Healthy/control	7.033	7.433	7.65	7.833	8.1	11.2	11.817	12.283	1675.4
	15	11/20/2018	Lab x Mastif susp	S	Healthy/control	4.5	7.017	8.15	8.817	9.4	9.7	10.033	10.217	1739.6
	16	11/21/2018	Labrador R	S	Healthy/control	3.733	3.983	4.517	4.7	4.9	5.033	5.167	5.317	2040.6

Case Data

PL-Mid	Sequence#	Date	Breed	Sex	Status	10.0 (kPa)	20.0 (kPa)	30.0 (kPa)	40.0 (kPa)	50.0 (kPa)	60.0 (kPa)	AUC	
	17	12/4/2018	G.Shepard	M	Bleeding	0	0	0	0	0	0	14.9	Scott Syndorome
	18	12/11/2018	mix	S	Post ope spay	8.283	9.183	0	0	0	0	52.6	spay
	19	12/112018	mix (Pit bull)	S	Post ope spay	1.6	2.3	4.117	4.967	6.8	0	322	spay
		12/12/2018	mix (Pit bull)	S	Post ope spay	0	0	0	0	0	0	1.2	
	20	12/12/2018	mix	C	Bleeding	2.8	3.283	3.85	4.2	5.417	5.717	372	
	21	12/13/2018	mix	C	Post ope cast	0	0	0	0	0	0	10.2	cast
	22	1/8/2019	Boston Terrier	S	Bleeding	0.6	0.617	5.5	5.933	6.55	7.517	290.9	Hemorragic Diarrehea
	23	1/10/2019	Shepherd	M	Bleeding	1.683	1.9	2.017	2.283	2.867	4.783	438.6	HemoA
	24	1/10/2019	Doberman	F	Bleeding	2.083	2.233	2.733	5.033	6.167	6.617	367.4	vWD type1 carrier
	25	1/10/2019	Doberuman	M	Bleeding	0	0	0	0	0	0	35.8	vWD type1 carrier

	26	1/16/2019	Doberuman	M	Bleeding	0	0	0	0	0	0	1	vWD susp
	27	1/17/2019	Shepherd	M	Bleeding	2.3	2.5	3.217	6.7	7.367	8.283	302	HemoA
	28	1/25/2019	Shetland	S	Bleeding	6.483	0	0	0	0	0	31.8	vWD type3
	29	2/4/2019	Doberman	F	Bleeding	3.35	3.5	3.65	5.117	6.817	7.35	313.1	
	30	2/6/2019	Mix	S	Post ope	0	0	0	0	0	0	4.7	spay
	31	2/6/2019	Mix	S	Post ope	3.75	3.933	4.2	4.383	4.933	6.517	329	spay
	32	2/7/2019	Mix	S	Post ope	0	0	0	0	0	0	7.2	spay
	33	2/13/2019	Mix	S	Post ope	5.55	5.733	5.867	6.15	6.417	8.067	223.9	spay
	34	2/14/2019	Mix	S	Post ope	2.15	2.3	2.533	2.95	4.183	4.6	423.7	spay
	35	2/14/2019	Mix	S	Post ope	3.017	3.267	3.533	3.717	3.883	5.6	376.2	spay
	36	2/15/2019	G.Shepherd	C	Bleeding	2.933	3.017	3.35	3.483	3.917	4.083	402.3	
	37	2/20/2019	Doberman	F	Bleeding	5.867	6.283	6.517	7.683	8.633	9.033	178.8	
	38	2/26/2019	Mix (G.Shepherd)	S	Post ope	6.8	6.933	7.083	7.167	7.317	7.467	187.2	spay mammary mass removal
	39	2/28/2019	Mix	S	Post ope	8.2	8.767	9.55	0	0	0	49.3	spay
	40	2/28/2019	Mix	S	Post ope	2.817	2.933	3.15	3.883	6.067	6.45	348.4	spay
	41	3/18/2019	Mix	M	Bleeding	1.5	1.85	3.983	7.033	0	0	220.9	abdominal hemorrage with Liver mass
PL-	17	12/4/2018	G.Shepard	M	Bleeding	8.85	9.233	9.667	10	0	0	41	Scott

Low													Syndorome
	18	12/11/2018	mix	S	Post ope spay	9.45	9.933	0	0	0	0	16.9	spay
	19	12/11/2018	mix (Pit bull)	S	Post ope spay	0	0	0	0	0	0	42.5	spay
		12/12/2018	mix (Pit bull)	S	Post ope spay	0	0	0	0	0	0	0.8	
	20	12/12/2018	mix	C	Bleeding	2.117	2.4	2.767	4.083	4.133	0	192.6	
	21	12/13/2018	mix	C	Post ope cast	0	0	0	0	0	0	17.4	cast
	22	1/8/2019	Boston Terrier	S	Bleeding	0.917	2.883	3.117	3.45	0	0	61.2	Hemorragic Diarrehea
	23	1/10/2019	Shepherd	M	Bleeding	2.167	2.317	2.65	2.967	3.45	4.133	437.4	HemoA
	24	1/10/2019	Doberman	F	Bleeding	2.267	2.467	3.05	7.7	10.083	0	225.2	vWD type1 carrier
	25	1/10/2019	Doberuman	M	Bleeding	5.05	5.4	6.8	8.533	0	0	132.6	vWD type1 carrier
	26	1/16/2019	Doberuman	M	Bleeding	0	0	0	0	0	0	1	vWD susp
	27	1/17/2019	Shepherd	M	Bleeding	2.3	2.5	3.217	6.7	7.367	8.283	302	HemoA
	28	1/25/2019	Shetland	S	Bleeding	2.617	7.85	0	0	0	0	75.3	vWD type3
	29	2/4/2019	Doberman	F	Bleeding	2.783	3	3.783	5.767	9.317	9.9	248.2	
	30	2/6/2019	Mix	S	Post ope	6.767	7.15	8.4	9.567	0	0	87.2	spay
	31	2/6/2019	Mix	S	Post ope	5.9	6.283	6.983	7.683	0	0	125.7	spay

	32	2/7/2019	Mix	S	Post ope	0	0	0	0	0	0	5.9	spay
	33	2/13/2019	Mix	S	Post ope	3.85	4.067	4.25	4.483	5.4	6.183	324.1	spay
	34	2/14/2019	Mix	S	Post ope	2.7	2.767	2.933	3	6.367	6.533	349.9	spay
	35	2/14/2019	Mix	S	Post ope	5.767	6.933	8.217	8.833	9.65	0	126.9	spay
	36	2/15/2019	G.Shepherd	C	Bleeding	3.35	3.55	3.733	3.867	4.233	5.133	366.9	
	37	2/20/2019	Doberman	F	Bleeding	4.85	5.067	5.767	6.767	7.933	10	199.4	
	38	2/26/2019	Mix (G.Shepherd)	S	Post ope	3.283	3.35	3.417	3.633	3.717	3.883	398.9	spay mammary mass removal
	39	2/28/2019	Mix	S	Post ope	0	0	0	0	0	0	8.4	spay
	40	2/28/2019	Mix	S	Post ope	4.55	4.783	5.283	8.217	9.217	9.983	192.3	spay
	41	3/18/2019	Mix	M	Bleeding	0.9	1.267	1.75	5.517	0	0	150.8	abdominal hemorrage with Liver mass

AR-High	Sequence#	Date	Breed	Sex	Status	10.0 (kPa)	20.0 (kPa)	30.0 (kPa)	40.0 (kPa)	50.0 (kPa)	60.0 (kPa)	70.0 (kPa)	80.0 (kPa)	AUC	
	17	12/4/2018	G.Shepard	M	Bleeding	0	0	0	0	0	0	0	0	36.2	Scott Syndorome
	18	12/11/2018	mix	S	Post opespay	3.833	4.783	5.017	5.367	5.7	5.9	6.4	6.517	1985.7	spay
	19	12/11 2018	mix (Pit bull)	S	Post opespay	10.083	10.383	10.517	10.667	11.1	11.167	11.333	11.417	1552.8	spay
		12/12/2018	mix (Pit bull)	S	Post opespay	6.533	6.9	7.167	7.4	7.65	7.783	7.933	8.083	1826.2	
	20	12/12/2018	mix	C	Bleeding	7.217	8	8.633	9.117	9.583	10.183	10.733	10.9	1691.6	
	21	12/13/2018	mix	C	Post opecast	5.017	5.883	6.117	6.433	6.617	6.767	6.883	7.233	1911.5	cast
	22	1/8/2019	Boston Terrier	S	Bleeding	5.3	5.85	6.4	6.617	7.05	8.283	8.467	8.633	1850.2	Hemorragic Diarrhea

	23	1/10/2019	Shepherd	M	Bleeding	7.517	8.067	8.533	8.9	9.167	9.417	9.65	9.983	1722.9	Hemo A
	24	1/10/2019	Doberman	F	Bleeding	10.433	11.4	11.817	12.033	12.25	12.483	12.95	13.3	1471.5	vWD type1 carrier
	25	1/10/2019	Doberuman	M	Bleeding	6.35	6.7	7.317	7.483	7.617	7.767	7.817	8.417	1831.7	vWD type1 carrier
	26	1/16/2019	Doberuman	M	Bleeding	14.567	15	15.967	16.233	16.35	16.933	17.367	17.6	1150	vWD susp
	27	1/17/2019	Shepherd	M	Bleeding	10.85	11.133	12.65	12.983	13.317	13.75	14.083	14.367	1389.8	Hemo A
	28	1/25/2019	Shetland	S	Bleeding	1.517	8.85	27.733	27.817	27.983	29.017	0	0	685.4	vWD type3
	29	2/4/2019	Doberman	F	Bleeding	6.7	7.35	8.05	8.517	8.9	9.117	9.367	9.567	1753.9	
	30	2/6/2019	Mix	S	Postope	4.667	5.183	5.417	5.75	5.867	5.983	6.083	6.183	1962.5	spay
	31	2/6/2019	Mix	S	Postope	4.633	4.833	5.117	5.3	5.417	5.533	5.6	5.7	1994.3	spay
	32	2/7/2019	Mix	S	Postope	2.933	3.133	3.617	3.8	4.033	4.25	4.383	4.5	2109.7	spay
	33	2/13/2019	Mix	S	Postope	4.767	5.433	5.75	6.1	6.417	6.683	6.95	7.083	1933.6	spay

	34	2/14/2019	Mix	S	Post ope	2.95	3.267	3.483	3.6	3.75	3.867	3.983	4.067	2125.3	spay
	35	2/14/2019	Mix	S	Post ope	4.233	4.55	4.717	5.2	6.033	6.333	6.6	6.817	1973.9	spay
	36	2/15/2019	G.Shepherd	C	Bleeding	4.233	4.617	4.917	5.817	6.15	6.317	6.5	6.633	1967.1	
	37	2/20/2019	Doberman	F	Bleeding	6.267	6.617	6.95	7.3	7.55	7.917	8.1	8.233	1831.2	
	38	2/26/2019	Mix (G.Shepherd)	S	Post ope	2.783	2.9	3	3.217	3.367	3.467	3.55	3.633	2152.6	spay mammary mass removal
	39	2/28/2019	Mix	S	Post ope	11.65	12.45	12.7	13.033	13.317	13.5	13.7	13.9	1397.3	
	40	2/28/2019	Mix	S	Post ope	3.733	3.95	4.25	4.683	4.833	5.233	5.533	5.767	2039.7	
	41	3/18/2019	Mix	M	Bleeding	7.85	12.25	13.067	13.967	14.833	15.467	16.367	16.833	1310.4	abdominal hemorrage with Liver

															mass
AR-Low	17	12/4/2018	G.Shepard	M	Bleeding	22.567	22.65	22.783	23.15	23.533	23.717	23.85	23.983	570.3	Scott Syndorome
	18	12/11/2018	mix	S	Post opespay	6.317	8.033	9.7	11.017	12.217	13.133	14.1	14.483	1565.3	spay
	19	12/11 2018	mix (Pit bull)	S	Post opespay	9.433	10.05	10.35	11.167	11.733	12.017	14.083	14.45	1494.9	spay
		12/12/2018	mix (Pit bull)	S	Post opespay	9.567	10.367	10.7	11	12.117	12.683	13.033	13.283	1508.7	
	20	12/12/2018	mix	C	Bleeding	7.6	9.3	10.75	11.583	12.05	12.367	12.533	12.767	1547.4	
	21	12/13/2018	mix	C	Post opecast	5.617	6.117	6.5	7	7.733	8.033	9.533	10.317	1815.3	cast
	22	1/8/2019	Boston Terrier	S	Bleeding	4.7	5.567	7.717	8.567	8.95	9.433	10.017	13.067	1725.8	Hemorragic Diarre

															hea
	23	1/10/2019	Shepherd	M	Bleeding	16.383	19.017	20.05	21.45	21.717	0	0	0	283.9	Hemo A
	24	1/10/2019	Doberman	F	Bleeding	5.583	6.817	7.367	8.05	9.333	9.7	10.05	10.217	1756	vWD type1 carrier
	25	1/10/2019	Doberuman	M	Bleeding	5.217	5.883	6.25	7.517	8.183	8.55	9.117	9.483	1828.9	vWD type1 carrier
	26	1/16/2019	Doberuman	M	Bleeding	14.8	15.55	15.933	18.583	18.917	19.267	19.567	19.783	1028.6	vWD susp
	27	1/17/2019	Shepherd	M	Bleeding	15.25	16.767	17.6	18.7	19.067	22.3	0	0	580.3	Hemo A
	28	1/25/2019	Shetland	S	Bleeding	5.133	6.883	8.667	12.967	0	0	0	0	768.3	vWD type3
	29	2/4/2019	Doberman	F	Bleeding	7.717	8.467	9.367	10.75	11.833	12.417	13.017	13.533	1570.9	
	30	2/6/2019	Mix	S	Postope	6.033	6.733	7.667	8.167	8.667	9.05	9.333	9.7	1776.8	spay
	31	2/6/2019	Mix	S	Postope	5.033	6.1	6.667	8.267	8.85	9.533	9.9	10.4	1790.3	spay
	32	2/7/2019	Mix	S	Postope	3.517	3.883	4.4	4.833	5.083	5.267	5.467	5.667	2039.6	spay

	33	2/13/2019	Mix	S	Post ope	8.5	9.967	11.567	12.133	12.85	13.45	14.65	15.117	1463.4	spay
	34	2/14/2019	Mix	S	Post ope	5	5.933	7.033	7.767	8.2	8.533	8.867	9.317	1822.5	spay
	35	2/14/2019	Mix	S	Post ope	5.133	5.9	6.35	6.967	7.2	7.333	7.517	10.583	1853.7	spay
	36	2/15/2019	G.Shepherd	C	Bleeding	6.367	7.817	9.117	9.65	10.083	10.35	10.65	11.917	1679.6	
	37	2/20/2019	Doberman	F	Bleeding	27.1	28.067	28.95	29.617	0	0	0	0	95.9	
	38	2/26/2019	Mix (G.Shepherd)	S	Post ope	3.133	3.483	3.833	4.117	4.433	4.683	4.917	5.133	2080.7	spay mammary mass removal
	39	2/28/2019	Mix	S	Post ope	8.167	8.983	9.233	10.783	11.167	11.5	13.1	14.083	1549.3	spay
	40	2/28/2019	Mix	S	Post ope	4.183	5.583	6.283	7.15	8.35	8.683	9.367	9.75	1837.6	spay
	41	3/18/2019	Mix	M	Bleeding	17.683	19.25	19.4	25.667	0	0	0	0	443.5	abdominal hemorrage

															with Liver mass

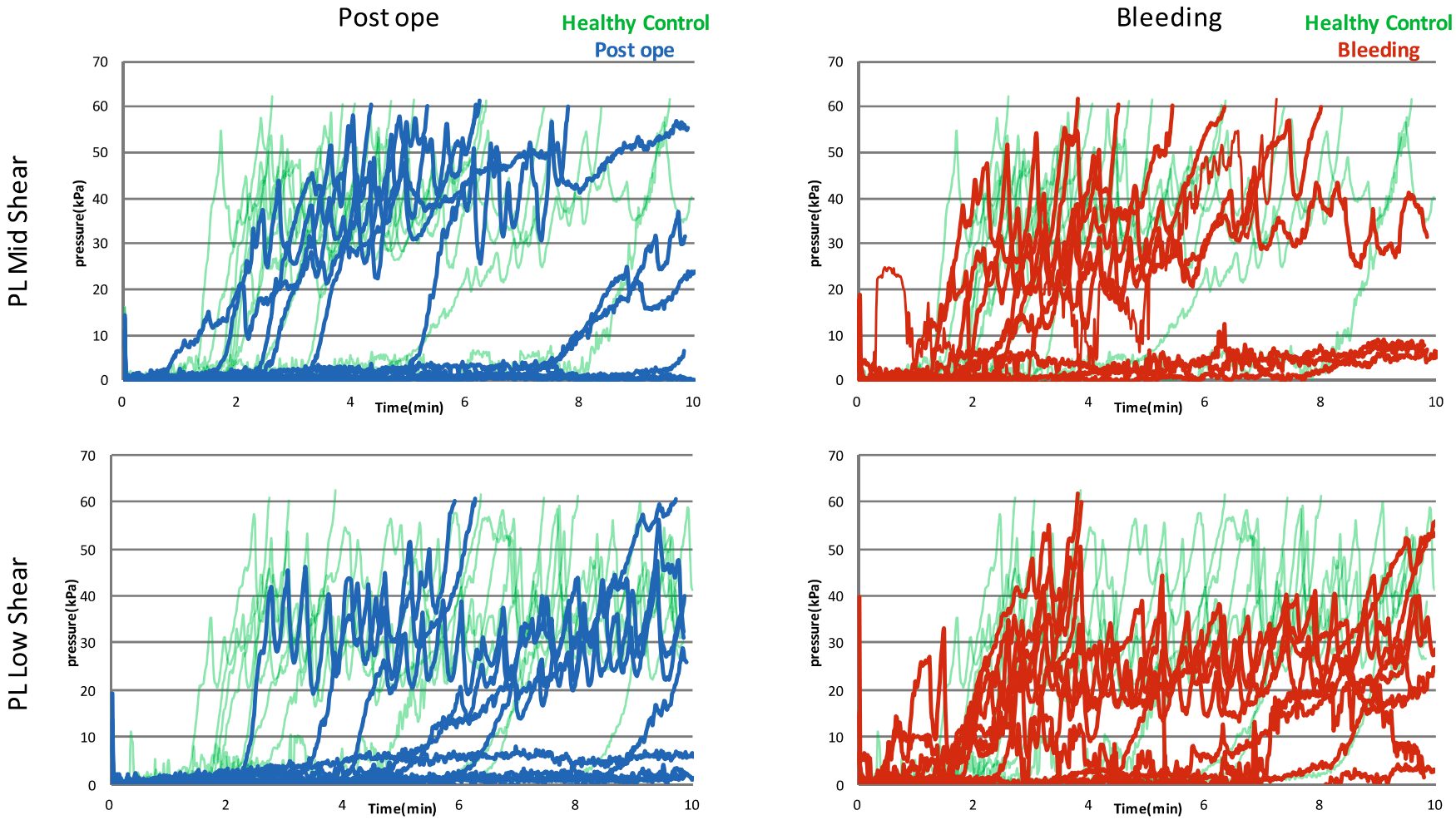
Post ope
Healthy Control
Post ope
Bleeding
Healthy Control
Bleeding
PL Mid Shear
PL Low Shear
pressure(kPa)
Time(min)
0
10
20
30
40
50
60
70
2
4
6
8

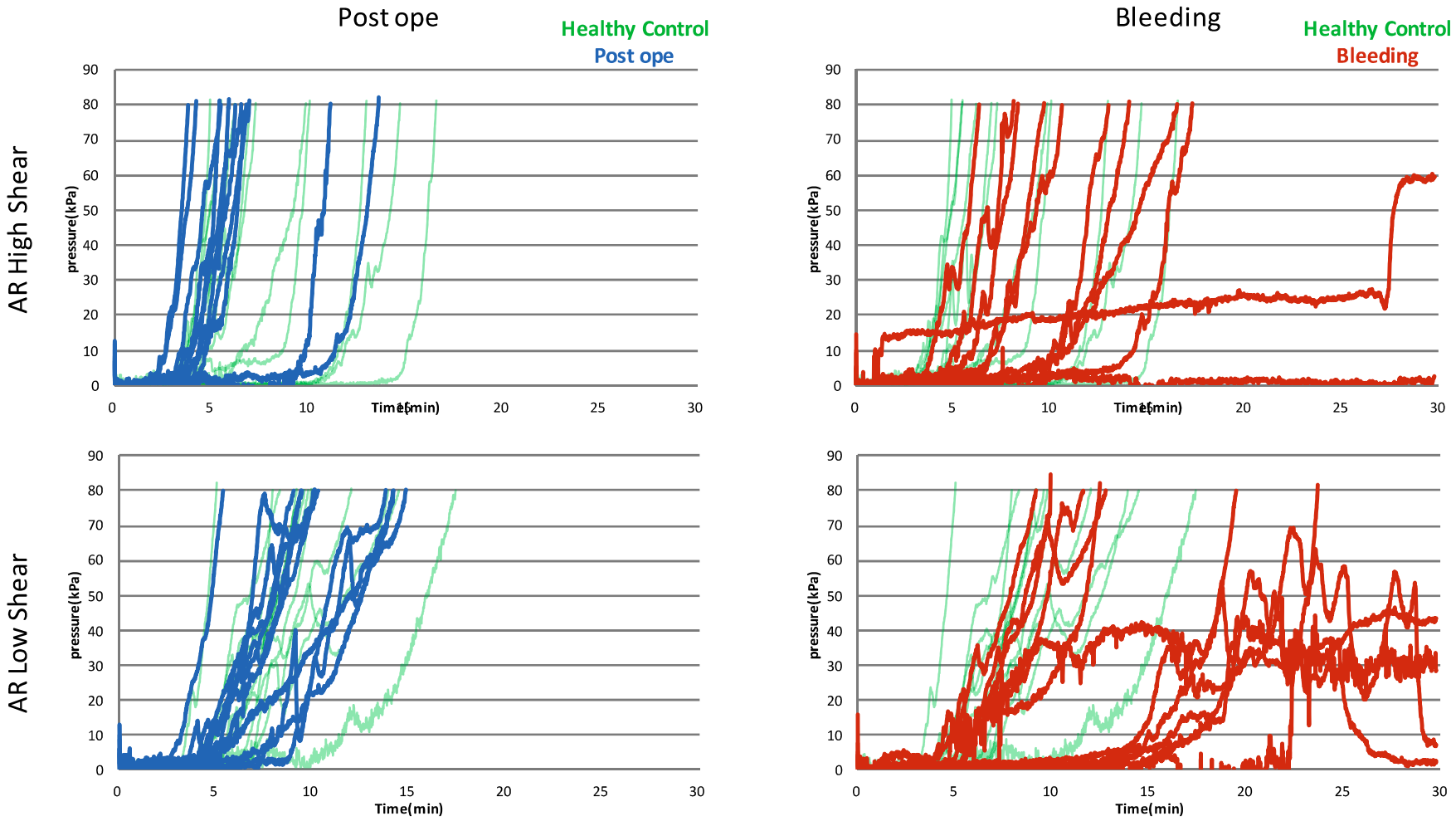
Post ope
Healthy Control
Post ope
Bleeding
Healthy Control
Bleeding
AR High Shear
AR Low Shear
pressure(kPa)
Time(min)
0
10
20
30
40
50
60
70
80
90
0
5
10
15
20
25
30

Bleeding: vWD

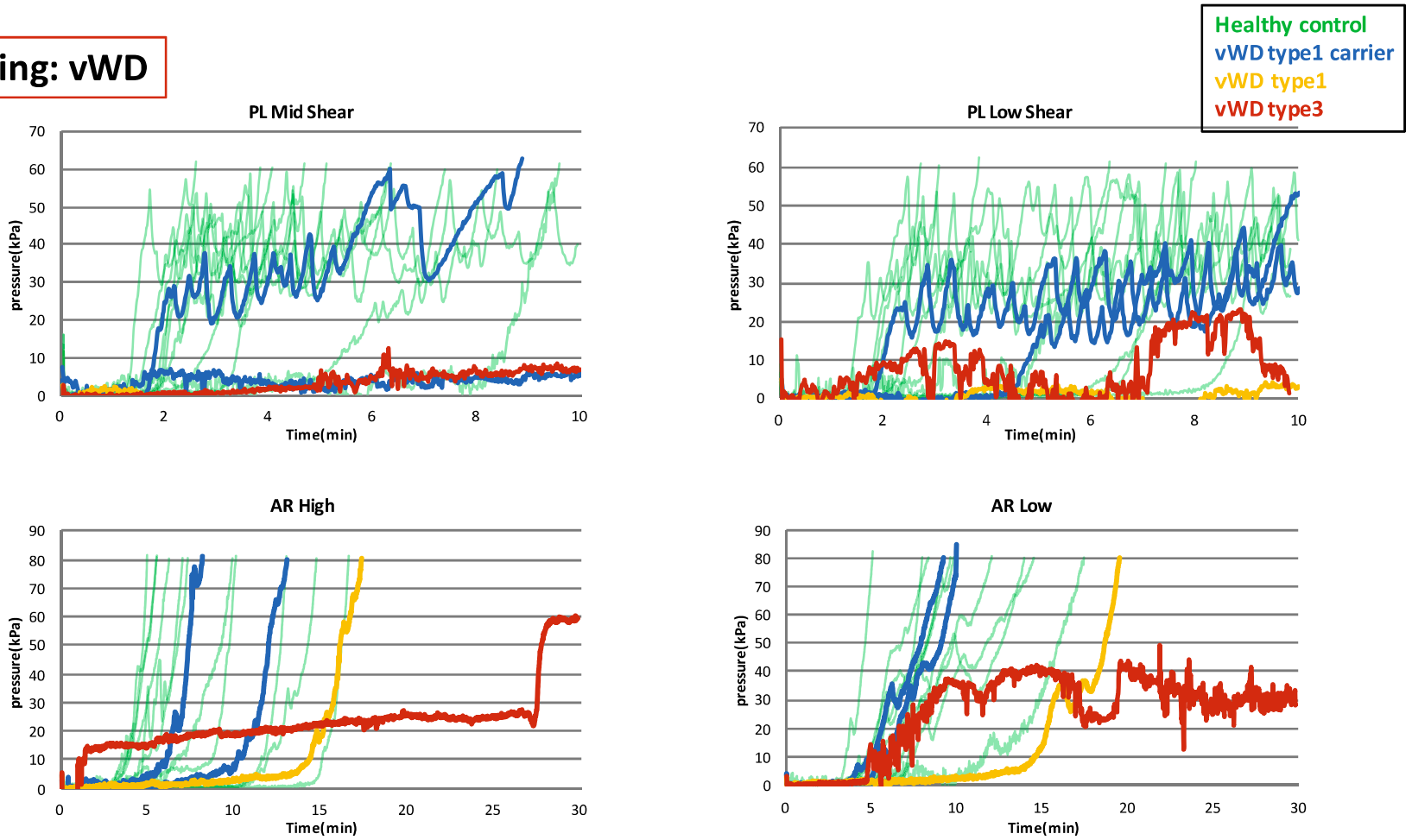

Bleeding: Hemophilia A

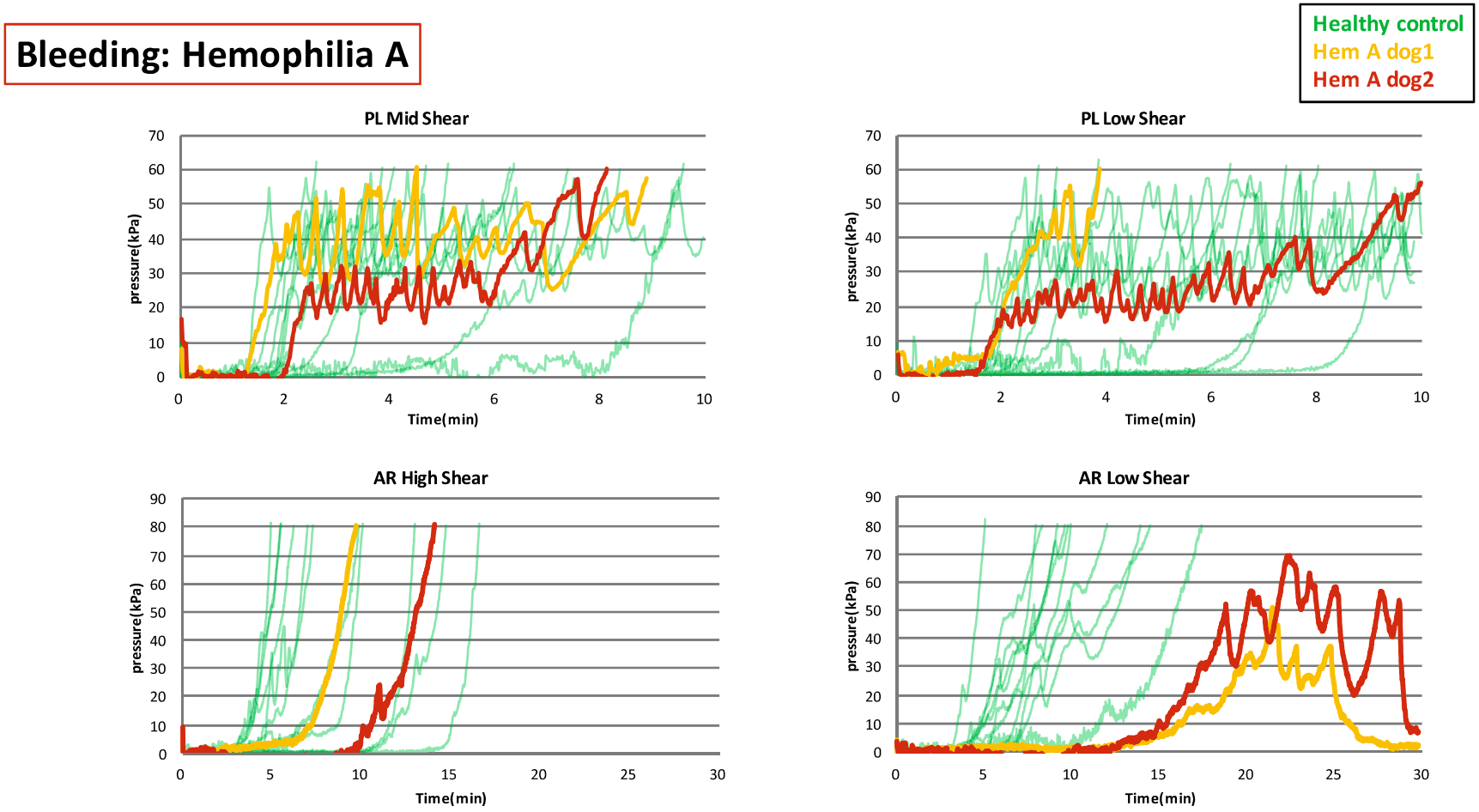

Bleeding: Hemophilia A

AR High Shear

Healty Dog

flow direction

Hem A dog1

Hem A dog2

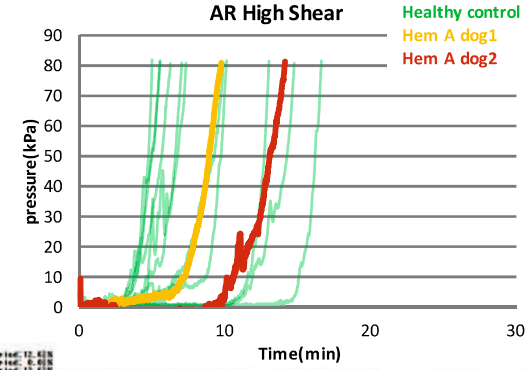

AR Low Shear

Healty Dog

flow direction

Hem A dog1

18min

21min

24min

27min

Hem A dog2

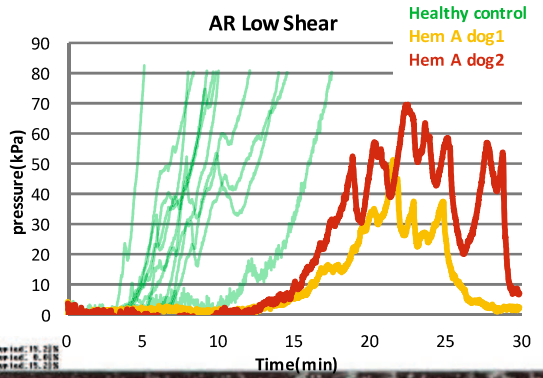

Bleeding: Scott Syndrome

Healthy control
Scott dog1 (non bleeding)
Scott dog2 (bleeding)

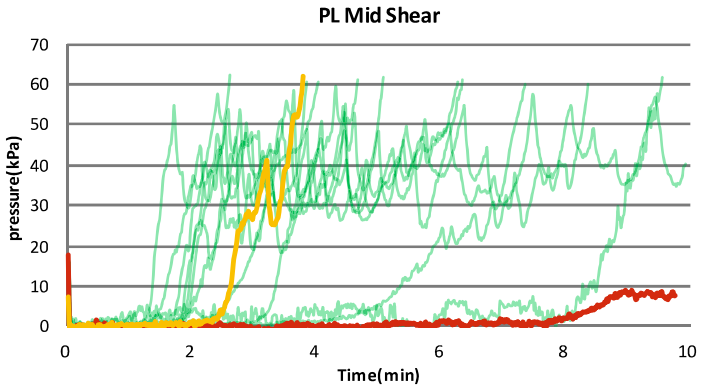

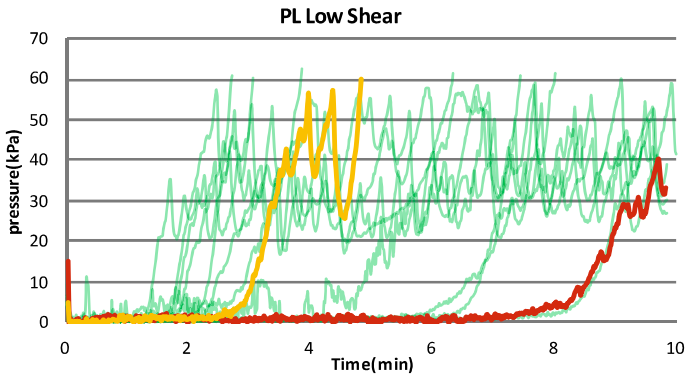

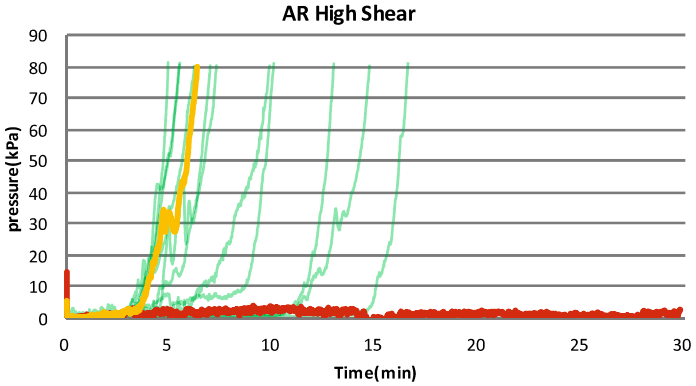

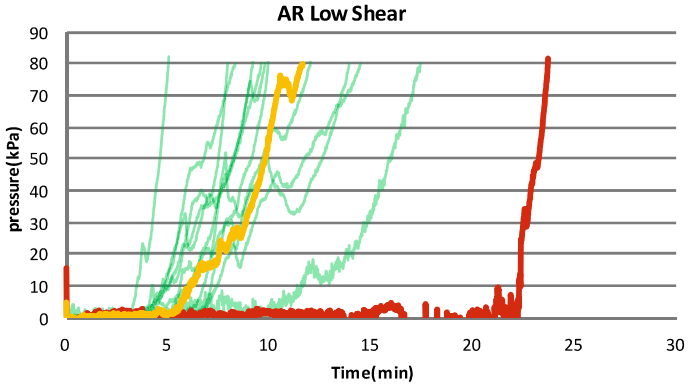

Bleeding: Mass

Healthy control
Scott dog1 (Hemangisarcoma)
Scott dog2 (hepatocellular carcinoma andhemangiosarcoma)

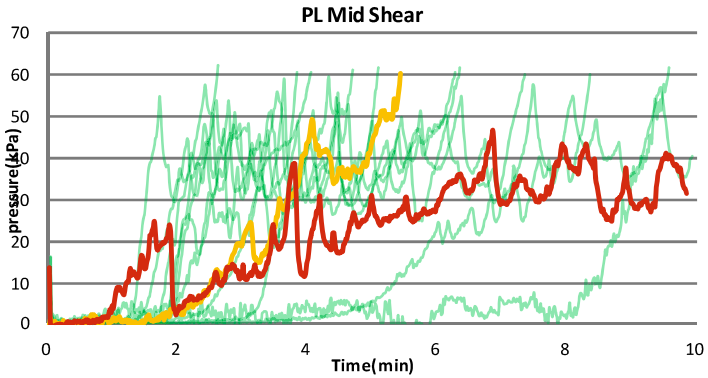

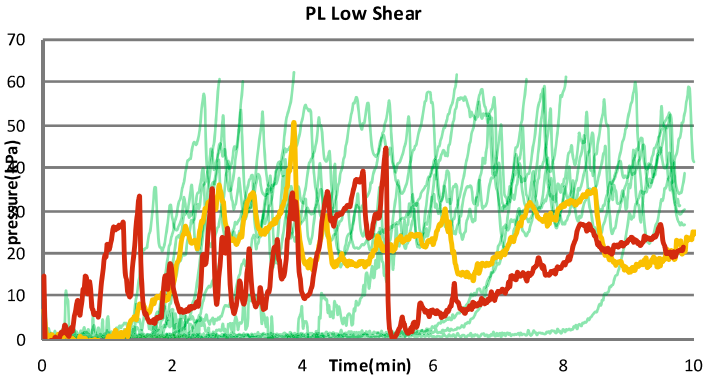

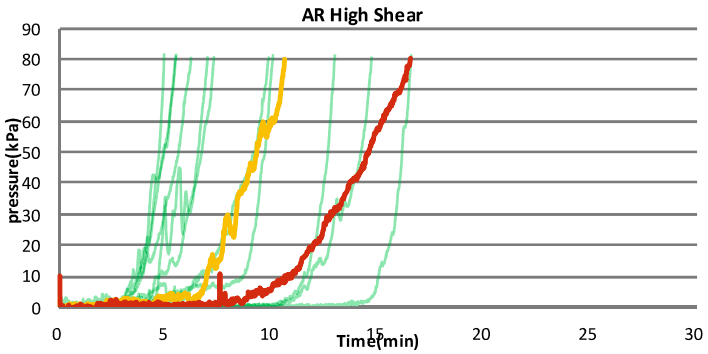

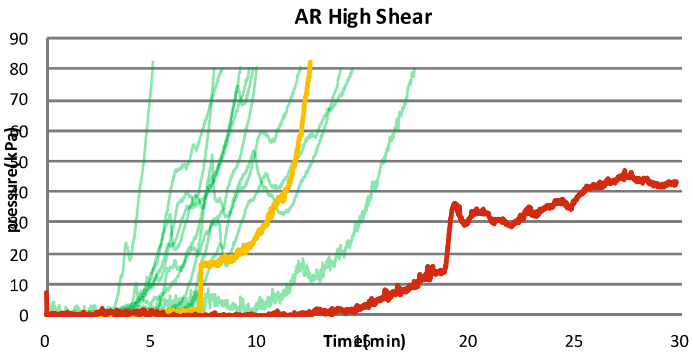

Bleeding: Acute Hemorrhagic Diarrhea Syndrome (AHDS)

Healthy control
Dog1 (AHDS)

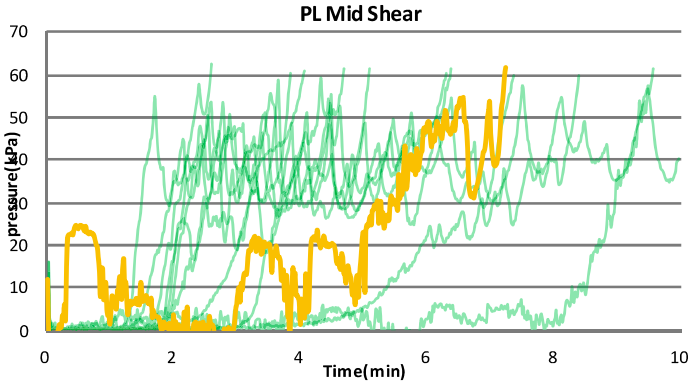

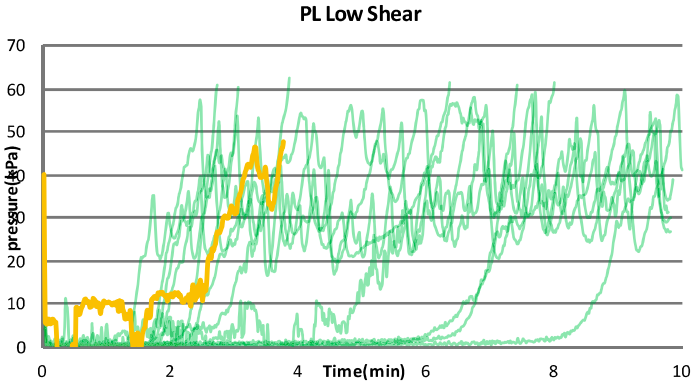

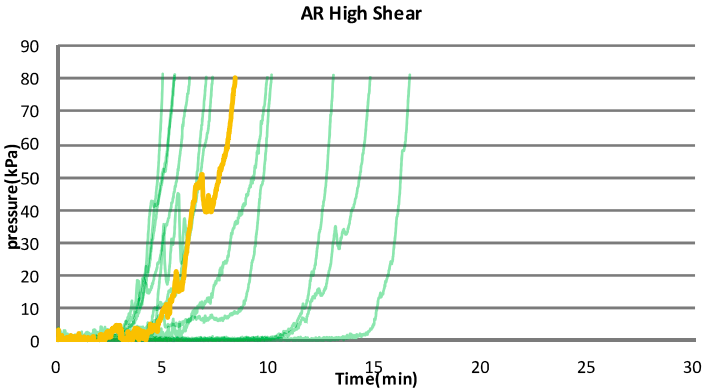

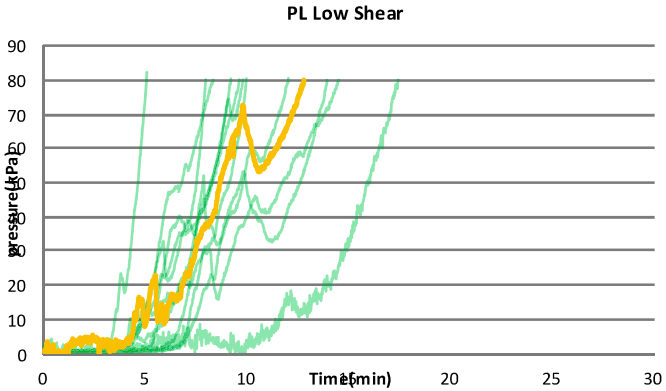

References

[1] R. C. Becker, “Cell-based models of coagulation: A paradigm in evolution,” *J. Thromb. Thrombolysis*, vol. 20, no. 1, pp. 65–68, 2005, doi: 10.1007/s11239-005-3118-3.

[2] M. Hoffman and D. M. Monroe, “A cell-based model of hemostasis,” *Thromb. Haemost.*, vol. 85, no. 6, pp. 958–965, 2001, doi: 10.1055/s-0037-1615947.

[3] M. Hoffman, “A cell-based coagulation factor Vlla and the role of,” *Blood Rev.*, vol. 17, pp. S1–S5, 2003.

[4] S. A. Smith, “The cell-based model of coagulation: State-Of-The-Art Review,” *J. Vet. Emerg. Crit. Care*, vol. 19, no. 1, pp. 3–10, 2009, doi: 10.1111/j.1476-4431.2009.00389.x.

[5] B. Wiinberg and A. T. Kristensen, “Thromboelastography in veterinary medicine,” *Semin. Thromb. Hemost.*, vol. 36, no. 7, pp. 747–756, 2010, doi: 10.1055/s-0030-1265291.

[6] A. Kol and D. L. Borjesson, “Application of thrombelastography/thromboelastometry to veterinary medicine,” *Vet. Clin. Pathol.*, vol. 39, no. 4, pp. 405–416, 2010, doi: 10.1111/j.1939-165X.2010.00263.x.

[7] B. Wiinberg *et al.*, “Tissue factor activated thromboelastography correlates to clinical signs of bleeding in dogs,” *Vet. J.*, 2009, doi: 10.1016/j.tvjl.2007.08.022.

[8] V. A. Bowbrick, D. P. Mikhailidis, and G. Stansby, “Value of thromboelastography in the assessment of platelet function,” *Clin. Appl. Thromb.*, vol. 9, no. 2, pp. 137–142, 2003, doi: 10.1177/107602960300900208.

[9] K. E. Jandrey, “Assessment of platelet function,” *J. Vet. Emerg. Crit. Care*, vol. 22, no. 1, pp. 81–98, 2012, doi: 10.1111/j.1476-4431.2011.00707.x.

[10] A. Srivastava and A. Kelleher, “Point-of-care coagulation testing,” *Contin. Educ. Anaesthesia, Crit. Care Pain*, vol. 13, no. 1, pp. 12–16, 2013, doi: 10.1093/bjaceaccp/mks049.

[11] Y. Yamaguchi *et al.*, “Studies of a microchip flow-chamber system to characterize whole blood thrombogenicity in healthy individuals,” *Thromb. Res.*, vol. 132, no. 2, pp. 263–270, 2013, doi: 10.1016/j.thromres.2013.05.026.

[12] K. Hosokawa *et al.*, “A novel automated microchip flow-chamber system to quantitatively evaluate thrombus formation and antithrombotic agents under blood flow conditions,” *J. Thromb. Haemost.*, vol. 9, no. 10, pp. 2029–2037, 2011, doi: 10.1111/j.1538-7836.2011.04464.x.

[13] K. Hosokawa *et al.*, “A microchip flow-chamber system for quantitative assessment of the platelet thrombus formation process,” *Microvasc. Res.*, vol. 83, no. 2, pp. 154–161, 2012, doi: 10.1016/j.mvr.2011.11.007.

[14] H. Minami, K. Nogami, K. Ogiwara, S. Furukawa, K. Hosokawa, and M. Shima, “Use of a microchip flow-chamber system as a screening test for platelet storage pool disease,” *Int. J. Hematol.*, vol. 102, no. 2, pp. 157–162, 2015, doi: 10.1007/s12185-015-1819-8.

[15] S. Ichikawa *et al.*, “Impact of total antithrombotic effect on bleeding complications in

patients receiving multiple antithrombotic agents," *Circ. J.*, vol. 83, no. 6, pp. 1309–1316, 2019, doi: 10.1253/circj.CJ-18-1236.

[16] H. Sugihara *et al.*, " Evaluation of the Antithrombotic Effects of Rivaroxaban and Apixaban Using the Total Thrombus-Formation Analysis System ® : In Vitro and Ex Vivo Studies ," *J. Clin. Med. Res.*, vol. 8, no. 12, pp. 899–907, 2016, doi: 10.14740/jocmr2773w.

[17] Y. Arima *et al.*, "Assessment of platelet-derived thrombogenicity with the total thrombus-formation analysis system in coronary artery disease patients receiving antiplatelet therapy," *J. Thromb. Haemost.*, vol. 14, no. 4, pp. 850–859, 2016, doi: 10.1111/jth.13256.

[18] K. Hosokawa *et al.*, "Antithrombotic effects of PAR1 and PAR4 antagonists evaluated under flow and static conditions," *Thromb. Res.*, vol. 133, no. 1, pp. 66–72, 2014, doi: 10.1016/j.thromres.2013.10.037.

[19] K. Kaikita, K. Hosokawa, J. R. Dahlen, and K. Tsujita, "Total Thrombus-Formation Analysis System (T-TAS): Clinical Application of Quantitative Analysis of Thrombus Formation in Cardiovascular Disease," *Thromb. Haemost.*, vol. 19, no. 10, pp. 1554–1562, 2019, doi: 10.1055/s-0039-1693411.

[20] T. Mitsuse *et al.*, "Total Thrombus-Formation Analysis System can Predict 1-Year," pp. 215–225, 2020.

[21] M. Ito *et al.*, "Total Thrombus-formation Analysis System (T-TAS) can predict periprocedural bleeding events in patients undergoing catheter ablation for atrial

fibrillation," *J. Am. Heart Assoc.*, vol. 5, no. 1, pp. 1–12, 2016, doi: 10.1161/JAHA.115.002744.

[22] V. Daidone *et al.*, "Usefulness of the Total Thrombus-Formation Analysis System (T-TAS) in the diagnosis and characterization of von Willebrand disease," *Haemophilia*, vol. 22, no. 6, pp. 949–956, 2016, doi: 10.1111/hae.12971.

[23] K. Nogami *et al.*, "Assessing the clinical severity of type 1 von Willebrand disease patients with a microchip flow-chamber system," *J. Thromb. Haemost.*, vol. 14, no. 4, pp. 667–674, 2016, doi: 10.1111/jth.13273.

[24] R. Al Ghaithi *et al.*, "Evaluation of the Total Thrombus-Formation System (T-TAS): application to human and mouse blood analysis," *Platelets*, vol. 30, no. 7, pp. 893–900, 2019, doi: 10.1080/09537104.2018.1535704.

[25] et al Ito T, Nagasato T, Nakashima T, Yamashita H, Matsuoka H, Hosokawa K, "Analyzing in vitro platelet thrombus formation of patients with essential thrombocythemia under blood flow conditions," *J Thromb Haemost*, vol. 13, p. 652, 2015.

[26] M. B. Brooks and J. L. Catalfamo, "Current Diagnostic Trends in Coagulation Disorders Among Dogs and Cats," *Vet. Clin. North Am. - Small Anim. Pract.*, vol. 43, no. 6, pp. 1349–1372, 2013, doi: 10.1016/j.cvsm.2013.07.003.

[27] J. Herring and M. McMichael, "Diagnostic Approach to Small Animal Bleeding Disorders," *Top. Companion Anim. Med.*, vol. 27, no. 2, pp. 73–80, 2012, doi:

10.1053/j.tcam.2012.07.004.

[28] K. Hosokawa *et al.*, “Plasminogen activator inhibitor type 1 in platelets induces thrombogenicity by increasing thrombolysis resistance under shear stress in an in-vitro flow chamber model,” *Thromb. Res.*, vol. 146, pp. 69–75, 2016, doi: 10.1016/j.thromres.2016.09.002.

[29] K. Ogiwara, K. Nogami, K. Hosokawa, T. Ohnishi, T. Matsumoto, and M. Shima, “Comprehensive evaluation of haemostatic function in von Willebrand disease patients using a microchip-based flow chamber system,” *Haemophilia*, vol. 21, no. 1, pp. 71–80, 2015, doi: 10.1111/hae.12610.

[30] M. Yamazaki *et al.*, “Measurement of residual platelet thrombogenicity under arterial shear conditions in cerebrovascular disease patients receiving antiplatelet therapy,” *J. Thromb. Haemost.*, vol. 14, no. 9, pp. 1788–1797, 2016, doi: 10.1111/jth.13391.

[31] S. Yamada *et al.*, “Comparison of chronological changes in blood characteristics in the atrium and peripheral vessels after the development of non-valvular atrial fibrillation,” *Thromb. Res.*, vol. 171, no. May, pp. 31–37, 2018, doi: 10.1016/j.thromres.2018.09.040.

[32] S. Yamada *et al.*, “Comparison between blood coagulability in the intra-atrial and peripheral regions during the acute phase after rapid atrial pacing,” *Exp. Anim.*, vol. 68, no. 2, pp. 137–146, 2019, doi: 10.1538/expanim.18-0100.

[33] K. Hosokawa *et al.*, “Analysing responses to aspirin and clopidogrel by measuring platelet

thrombus formation under arterial flow conditions," *Thromb. Haemost.*, vol. 109, no. 1, pp. 102–111, 2013, doi: 10.1160/TH12-06-0441.

[34] B. M. Brainard and A. J. Brown, "Defects in Coagulation Encountered in Small Animal Critical Care," *Vet. Clin. North Am. - Small Anim. Pract.*, vol. 41, no. 4, pp. 783–803, 2011, doi: 10.1016/j.cvsm.2011.04.001.

[35] M. B. Brooks, T. Stokol, and J. L. Catalfamo, "Comparative Hemostasis: Animal Models and New Hemostasis Tests," *Clin. Lab. Med.*, vol. 31, no. 1, pp. 139–159, 2011, doi: 10.1016/j.cll.2010.10.009.

[36] H. Yaoi, Y. Shida, K. Ogiwara, K. Hosokawa, M. Shima, and K. Nogami, "Role of red blood cells in the anemia-associated bleeding under high shear conditions," *Haemophilia*, vol. 23, no. 5, pp. 750–758, 2017, doi: 10.1111/hae.13252.

[37] Y. Sakamoto, H. Koami, and T. Miike, "Monitoring the coagulation status of trauma patients with viscoelastic devices," *J. Intensive Care*, vol. 5, no. 1, pp. 1–11, 2017, doi: 10.1186/s40560-016-0198-4.

[38] S. Yamada, R. Fukushima, T. Nagasato, N. Miura, and A. Cardiovascular, "Novel Thrombogenicity Examination of Whole Blood : Total Thrombus- Formation Analysis System in Dogs (Abstract HM16)," pp. 2017–2018, 2017.

[39] F. Gentilini and M. E. Turba, "Two novel real-time PCR methods for genotyping the von Willebrand disease type I mutation in Doberman Pinscher dogs," *Vet. J.*, vol. 197, no. 2,

pp. 457–460, 2013, doi: 10.1016/j.tvjl.2013.02.023.

[40] M. Brooks, S. Raymond, and J. Catalfamo, “Plasma von Willebrand factor antigen concentration as a predictor of von Willebrand’s disease status in German Wirehaired Pointers,” *J. Am. Vet. Med. Assoc.*, vol. 209, no. 5, pp. 930–933, 1996.

[41] M. E. Aslanian, C. R. Sharp, E. A. Rozanski, A. M. de Laforcade, M. Rishniw, and M. B. Brooks, “Clinical outcome after diagnosis of hemophilia a in dogs,” *J. Am. Vet. Med. Assoc.*, vol. 245, no. 6, pp. 677–683, 2014, doi: 10.2460/javma.245.6.677.

[42] D. G. Feldman, M. B. Brooks, and W. J. Dodds, “Hemophilia B (factor IX deficiency) in a family of German Shepherd Dogs,” *J. Am. Vet. Med. Assoc.*, vol. 206, no. 12, pp. 1901–1905, 1995.

[43] M. B. Brooks, J. L. Catalfamo, R. Macnguyen, D. Tim, S. Fancher, and J. A. Mccardle, “A TMEM16F point mutation causes an absence of canine platelet TMEM16F and ineffective activation and death-induced phospholipid scrambling,” *J. Thromb. Haemost.*, vol. 13, no. 12, pp. 2240–2252, 2015, doi: 10.1111/jth.13157.

[44] D. J. Fletcher, E. A. Rozanski, B. M. Brainard, A. M. de Laforcade, and M. B. Brooks, “Assessment of the relationships among coagulopathy, hyperfibrinolysis, plasma lactate, and protein C in dogs with spontaneous hemoperitoneum,” *J. Vet. Emerg. Crit. Care*, vol. 26, no. 1, pp. 41–51, 2016, doi: 10.1111/vec.12346.

[45] F. Mortier, K. Strohmeyer, K. Hartmann, and S. Unterer, “Acute haemorrhagic diarrhoea

syndrome in dogs: 108 cases," *Vet. Rec.*, vol. 176, no. 24, p. 627, 2015, doi: 10.1136/vr.103090.

[46] C. M. Whitton, D. Sands, A. R. Hubbard, and P. J. Gaffney, "A collaborative study to establish the 2nd International Standard for Fibrinogen, Plasma.," *Thromb. Haemost.*, vol. 84, no. 2, pp. 258–262, Aug. 2000.

[47] I. B. Johnstone, "Plasma von Willebrand factor-collagen binding activity in normal dogs and in dogs with von Willebrand's disease," *J. Vet. Diagnostic Investig.*, vol. 11, no. 4, pp. 308–313, 1999, doi: 10.1177/104063879901100402.

[48] R. Goggs, B. Wiinberg, M. Kjelgaard-Hansen, and D. L. Chan, "Serial assessment of the coagulation status of dogs with immune-mediated haemolytic anaemia using thromboelastography," *Vet. J.*, vol. 191, no. 3, pp. 347–353, 2012, doi: 10.1016/j.tvjl.2011.03.015.

[49] B. Wiinberg, A. L. Jensen, R. Rojkjaer, P. Johansson, M. Kjelgaard-Hansen, and A. T. Kristensen, "Validation of human recombinant tissue factor-activated thromboelastography on citrated whole blood from clinically healthy dogs," *Vet. Clin. Pathol.*, vol. 34, no. 4, pp. 389–393, 2005, doi: 10.1111/j.1939-165X.2005.tb00066.x.

[50] A. De Laforcade, R. Goggs, and B. Wiinberg, "Systematic evaluation of evidence on veterinary viscoelastic testing Part 3: Assay activation and test protocol," *J. Vet. Emerg. Crit. Care*, vol. 24, no. 1, pp. 37–46, 2014, doi: 10.1111/vec.12147.

[51] R. Goggs *et al.*, "Partnership on Rotational ViscoElastic Test Standardization (PROVETS): Evidence-based guidelines on rotational viscoelastic assays in veterinary medicine," *J. Vet. Emerg. Crit. Care*, vol. 24, no. 1, pp. 1–22, 2014, doi: 10.1111/vec.12144.

[52] V. Allegret, M. Dunn, and C. Bédard, "Monitoring unfractionated heparin therapy in dogs by measuring thrombin generation," *Vet. Clin. Pathol.*, vol. 40, no. 1, pp. 24–31, 2011, doi: 10.1111/j.1939-165X.2011.00282.x.

[53] W. L. Chandler and M. Roshal, "Optimization of plasma fluorogenic thrombin-generation assays," *Am. J. Clin. Pathol.*, vol. 132, no. 2, pp. 169–179, 2009, doi: 10.1309/AJCP6AY4HTRAAJFQ.

[54] M. Sugimoto *et al.*, "Mural thrombus generation in type 2A and 2B von Willebrand disease under flow conditions," *Blood*, vol. 101, no. 3, pp. 915–920, 2003, doi: 10.1182/blood-2002-03-0944.

[55] S. Tsuji, M. Sugimoto, S. Miyata, M. Kuwahara, S. Kinoshita, and A. Yoshioka, "Real-time analysis of mural thrombus formation in various platelet aggregation disorders: Distinct shear-dependent roles of platelet receptors and adhesive proteins under flow," *Blood*, vol. 94, no. 3, pp. 968–975, 1999, doi: 10.1182/blood.v94.3.968.415a13_968_975.

[56] A. Michels, L. L. Swystun, J. Mewburn, S. Albánez, and D. Lillicrap, "Investigating von willebrand factor pathophysiology using a flow chamber model of von willebrand factor-platelet string formation," *J. Vis. Exp.*, vol. 2017, no. 126, pp. 1–9, 2017, doi:

10.3791/55917.

[57] K. De Ceunynck, S. F. De Meyer, and K. Vanhoorelbeke, “Unwinding the von Willebrand factor strings puzzle,” *Blood*, vol. 121, no. 2, pp. 270–277, 2013, doi: 10.1182/blood-2012-07-442285.

[58] G. L. Salvagno and E. Berntorp, “Thrombin generation testing for monitoring hemophilia treatment: A clinical perspective,” *Semin. Thromb. Hemost.*, vol. 36, no. 7, pp. 780–790, 2010, doi: 10.1055/s-0030-1265295.

[59] A. Ferkau, S. Ecklebe, K. Jahn, S. Calmer, G. Theilmeier, and R. Mischke, “A dynamic flow-chamber-based adhesion assay to assess canine platelet-matrix interactions in vitro,” *Vet. Clin. Pathol.*, vol. 42, no. 2, pp. 150–156, 2013, doi: 10.1111/vcp.12035.

[60] A. Ferkau *et al.*, “Infection-associated platelet dysfunction of canine platelets detected in a flow chamber model,” *BMC Vet. Res.*, vol. 9, 2013, doi: 10.1186/1746-6148-9-112.

[61] R. M. Schoeman, M. Lehmann, and K. B. Neeves, “Flow chamber and microfluidic approaches for measuring thrombus formation in genetic bleeding disorders,” *Platelets*, vol. 28, no. 5, pp. 463–471, 2017, doi: 10.1080/09537104.2017.1306042.

[62] A. Rana, E. Westein, B. Niego, and C. E. Hagemeyer, “Shear-Dependent Platelet Aggregation: Mechanisms and Therapeutic Opportunities,” *Front. Cardiovasc. Med.*, vol. 6, no. September, pp. 1–21, 2019, doi: 10.3389/fcvm.2019.00141.

[63] L. E. Witter, E. J. Gruber, F. Z. X. Lean, and T. Stokol, “Evaluation of procoagulant tissue

factor expression in canine hemangiosarcoma cell lines," *Am. J. Vet. Res.*, vol. 78, no. 1, pp. 69–79, 2017, doi: 10.2460/ajvr.78.1.69.

[64] R. Mischke, P. Wohlsein, and H. A. Schoon, "Detection of fibrin generation alterations in dogs with haemangiosarcoma using resonance thrombography," *Thromb. Res.*, vol. 115, no. 3, pp. 229–238, 2005, doi: 10.1016/j.thromres.2004.08.012.

[65] A. S. Hammer, C. G. Couto, C. Swardson, and D. Getzy, "Hemostatic Abnormalities in Dogs With Hemangiosarcoma," *J. Vet. Intern. Med.*, vol. 5, no. 1, pp. 11–14, 1991, doi: 10.1111/j.1939-1676.1991.tb00923.x.

[66] S. Dunkley and P. Harrison, "Platelet activation can occur by shear stress alone in the PFA-100 platelet analyser," *Platelets*, vol. 16, no. 2, pp. 81–84, 2005, doi: 10.1080/09537100400010352.